TNO Built Environment and Geosciences

Oil and Gas
Princetonlaan 6
P.O. Box 80015
3508 TA Utrecht
The Netherlands

www.tno.nl

T +31 30 256 42 56
F +31 30 256 44 75
info-beno@tno.nl

TNO report

Determination of petrophysical properties from well logs of the offshore Terschelling Basin and southern Central North Sea Graben region (NCP-2A) of the Netherlands

Date	February 15, 2007
Author(s)	Benedictus, T.
Project colaborators	Rijkers, R.H.B., Witmans, N.
Assignor	
Project number	
Classification report	
Title	
Abstract	
Report text	
Appendices	
Number of pages	53 (incl. appendices)
Number of appendices	2

Summary

As part of TNO's thematic mapping programme of the Dutch offshore, this study focuses on calculation of petrophysical parameters, porosity in particular, of several potential reservoir levels of the NCP-2A region, such as of the Jurassic Schieland and Scruff Groups, the Upper Germanic Triassic Solling Fat Sandstone member, the Lower Detfurth and Volpriehausen Sandstone members of the Lower Germanic Triassic Group and the Upper Rotliegend Slochteren Formation. To this purpose available bulk density logs are used, permitting accurate quantification of porosity estimates. The bulk density logs were disregarded when their value was below 2.0 g/cm^3 (or below 2.2 g/cm^3 for litho-stratigraphic units of the Schieland Group rich in organic matter or coal layers) in order to neglect unwanted side-effects leading to overestimated porosity values.

Per litho-stratigraphic unit the distribution of matrix density measurements was investigated, generally resulting in normally distributed matrix densities with distinct mean values, which could be applied in the calculation. From resistivity measurements the mud filtrate density, i.e. the pore fluid density, was derived for many wells, while for the remaining ones the mean value from these calculations was used.

In order to be able to discriminate net from gross lithologies, the gamma ray log is employed. On the scale of litho-stratigraphic units the mean of maximum and minimum gamma ray log values was used to distinguish between sandstone or sandy siltstone and shaly lithologies. For known gas-bearing reservoirs, the calculated porosity from the bulk density log was corrected for the significantly lower density of gas using the neutron log. To this purpose first the neutron log, representing fresh water-filled, limestone porosity, was converted to porosity values for the specific lithologies and pore fluids.

The calculated values were averaged over net intervals the litho-stratigraphic units of interest resulting in single net porosity values for the individual units of specific wells. Detailed data is available as porosity logs for the investigated intervals and wells. As the exercise of porosity determination involves several uncertainties, at this stage it was believed that using this data for calculation of permeability values would not be opportune.

Contents

1 Introduction

As part of its advisory task for the Dutch Ministry of Economic Affairs TNO performed multiple mapping studies and survey interpretations with the purpose to attract further exploration activities in the Netherlands, especially offshore. Using data and information gathered by private operators the Netherlands Continental Platform (NCP) was mapped in the past. AT present TNO focuses in more detail on five areas that together comprise the Dutch offshore region. The results of various studies on these areas will be geographically represented by thematic properties, such as structural, depth and thickness maps and facies-property maps. The latter product gives insight in the spatial distribution of petrophysical properties with respect to different facies occurrences.

The NCP-2A region (figure 1) is the first of five areas that is mapped in detail starting 2006. It roughly comprises the southern part of the Central North Sea Graben and the Terschelling Basin situated immediately north of Terschelling

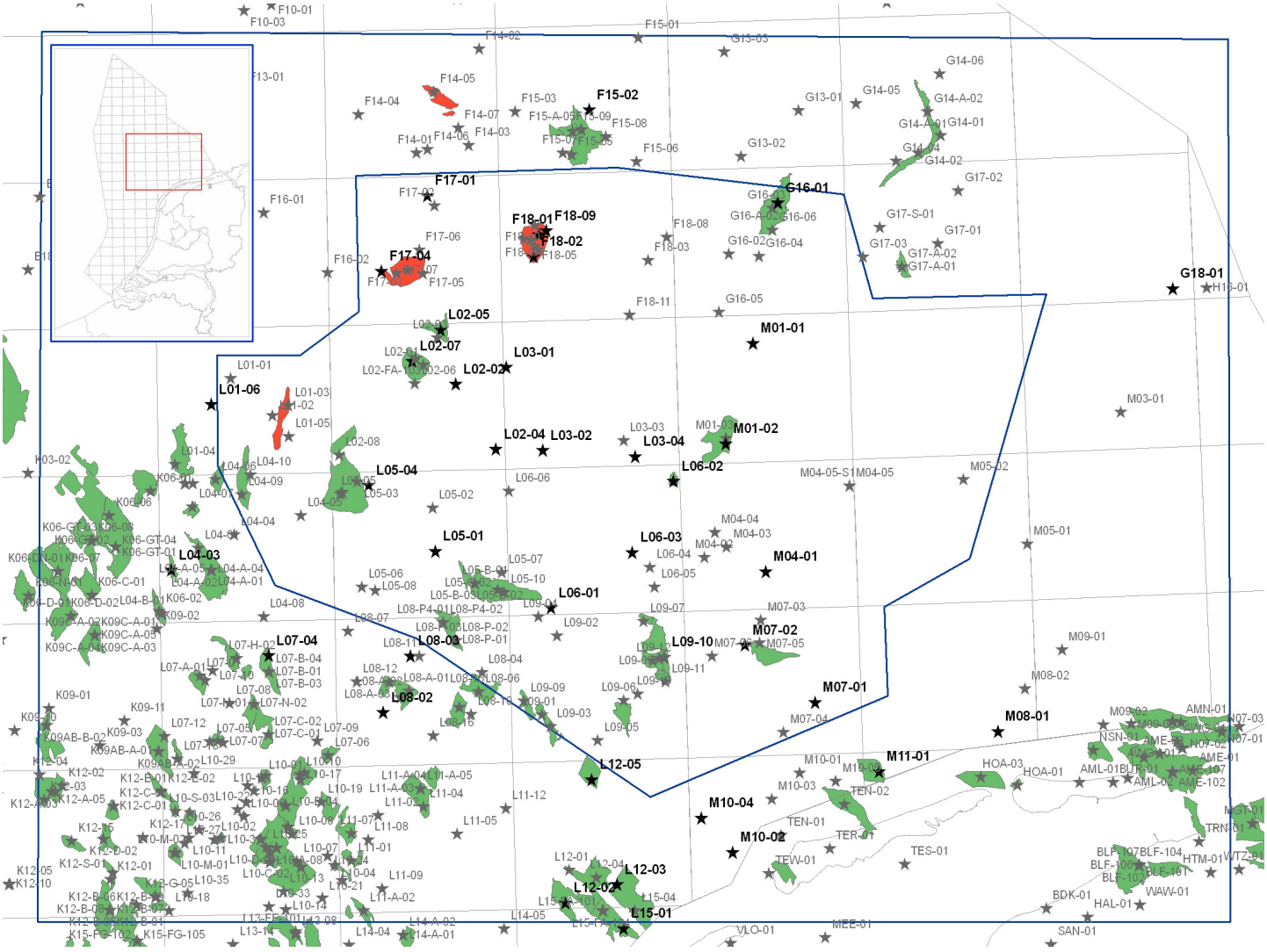

Figure 1. Dutch offshore NCP-2A region (in blue frame). Stars indicate wells; wells used in this study are printed in bold. Green shapes represent gas fields, red shapes represent oil fields.

Table 1. Conversion for official to proposed litho-stratigraphic nomenclature, based on Verreussel and Munsterman (2006). Modifications are printed in bold.

Official nomenclature		Proposed nomenclature (used in this study)	
Code	Litho-stratigraphic unit	Code	Litho-stratigraphic unit
SL	Schieland Group	SL	Schieland Group
SLC	Central Graben Subgroup	SLC	Central Graben Subgroup
SLCF	Friese Front Formation	SLCF	Friese Front Formation
SLCFM	**Main Friese Front Member**		
SLCFR	Rifgronden Member	SLCFR	Rifgronden Member
		SLCT	**Terschelling Formation**
SLCFO	**Oyster Ground Claystone Member**	**SLCTO**	**Oysterground Member**
SLCFT	Terschelling Sandstone Member	**SLCTS**	Terschelling Sandstone Member [1]
SG	**Scruff Group**	**SLS**	**Scruff Subgroup**
SGKI	**Kimmeridge Clay Formation**	**SLCK**	**Kimmeridge Formation** [2]
SGKIM	**Main Kimmeridge Clay Member**	**SLCK**	**Kimmeridge Formation** [2]
SGKIC	**Clay Deep Member**	**SLSD**	**Clay Deep Formation**
SGKIS	**Schill Grund Member**	**SLSS**	**Schill Grund Formation**
SGGS	Scruff Greensand Formation	**SLSG**	Scruff Greensand Formation
SGGSB	**Scruff Basal Sandstone Member**	**SLCTS**	**Terschelling Sandstone Member** [1]
SGGSA	**Scruff Argillaceous Member**	**SLCTA**	**Terschelling Argillaceous Member**
		SLCTB	**Terschelling Arenaceous Member**
SGGSP	Scruff Spiculite Member	**SLSGP**	Scruff Spiculite Member
SGGSS	Stortemelk Member	**SLSGS**	Stortemelk Member
RNSOM [3]	**Solling Middle Sandstone member**	**RNSOF**	**Solling Fat Sandstone member**

[1] *The proposed Terschelling Sandstone Member (SLCTS) comprises both the official Terschelling Sandstone Member (SLCFT) as well as the Scruff Basal Sandstone Member (SGGSB)*

[2] *The proposed Kimmeridge Formation (SLCK) comprises both the official Kimmeridge Clay Formation (SGKI) as well as the Main Kimmeridge Clay Member (SGKIM)*

[3] *The Solling Middle Sandstone member (RNSOM) is not officially defined in the nomenclature, but is typified in this study as an informal unit*

island off the Dutch coastline. This study focuses on the derivation of petrophysical properties, especially porosity, from available well log data in the NCP-2A region for several potential reservoir intervals of the Upper Jurassic Schieland and Scruff Groups, the Solling Fat Sandstone member of the Upper Germanic Triassic Group, the Lower Triassic Main Buntsandstein Subgroup and the Upper Rotliegend Group. The facies sequences in the Upper Jurassic Schieland and Scruff Groups in the Terschelling Basin and the southern Central North Sea Graben are interpreted in a simultaneously performed study based on available drilling cores from multiple wells (Stegers, 2006). These results will be combined with the results of the present study in a stage beyond this report.

Over the past decades many wells have been drilled in the Dutch offshore. For the NCP-2A region and its direct surroundings, therefore, a lot of information is

available from a fair amount of well logs. Sonic and gamma ray logs generally are present for most wells over large depth intervals. Bulk density and neutron logs have been recorded for many wells as well, but are typically of lesser vertical extent. Other sources of information have been drilling reports and drilling cores.

The official nomenclature of the Dutch subsurface recently has been updated (Abbink *et al*., 2006). However, this study was performed using a newly proposed litho-stratigraphic nomenclature for the Schieland and Scruff Groups, based on recently interpreted geo-biological markers (Verreussel and Munsterman, 2006). Despite the fact that this classification has not been approved in a late stage of this research project, descriptions in this report are still based on the proposed glossary and all litho-stratigraphic codes and names refer to the rejected proposed classification. Because the intended changes were not linear conversions of single units, it would be an elaborate process to transfer all calculations to another litho-stratigraphic subdivision. In order to be able to relate results to the correct units, table 1 contains a general conversion scheme. Furthermore, all final results are accompanied by the corresponding depth interval (measured depths).

2 Lithological descriptions from drilling cores

Cores are available for specific intervals of certain wells and are also used for measurement of porosity and matrix density. In order to gain insight in the lithology and the relation of lithology to well log expression, several litho-stratigraphic units have been investigated from drilling cores. Physical quality of the cores varies enormously as some cores are completely decayed, while others are fully intact. Hence, this forms a bounding condition in evaluation of the lithology. A more detailed description of Upper Jurassic Scruff and Schieland Group lithology and facies is reported by Stegers (2006).

2.1 Scruff Greensand Formation (SLSG)

The drilling core of depth interval between 2027-2045 m of well L06-03 does not provide much insight in the characteristics of the coinciding part of the Scruff Greensand Formation, other than the pervasive bioturbation of the entire interval and the presence of undefined fossils. Soil forming phenomena are abundant, especially in the upper part of the interval. The basal part enables better distinction of the fine grained and clay-like matrix material. A single cemented layer about 30 cm thick is present in the middle of the section and several cemented casts are recorded to be present in the lowest part.

2.2 Terschelling Sandstone Member (SLCTS)

Well L06-03 is also cored between 2095-2111 m depth, representing a sample of the Terschelling Sandstone Member from the Friese Front Formation of the Schieland Group. The upper meters of the interval show an alternation of heavily bioturbated material, rich in organic remnants and soil forming features, with several medium grained cemented sandstone layers, up to a meter individual thickness. The lower part of the sample forms an alternation of cemented medium to fine grained sandstone intervals and 20-70 cm thick layers consisting of very coarse grained sandstone with shell fragments and some black minerals, showing distinct parallel layering.
Drilling cores (2464-2497 m) from well L06-02 provide another example of the Terschelling Sandstone Member. The observed sequence consist of thick (up to 10 m) layers of medium sandstones showing evidence of intense bioturbation and minor faulting, alternated with heavily fractured beds of slumped and brecciated shell fragments, (very) coarse clasts and dark minerals in a clayey matrix. Furthermore, clean compacted fine to medium sandstone layers are present, displaying parallel laminae and local cementation.

2.3 Oysterground Member (SLCTO)

The lowest part (2497-2510 m) of the L06-02 drilling core samples the top of the underlying Oysterground Member. This unit consists of claystone containing abundant shell fragments and intercalated silty layers.

2.4 Friese Front Formation (SLCF)

In the lower part of Schieland Group's Friese Front Formation of well L06-03 two other intervals are sampled, i.e. 2054-2070 m and 2302-2323 m. Both drilling cores

show many intervals with soil forming features, bioturbation and breccias of brown gravel to pebble-sized clasts and reworked organic rich material and coal fragments. Typically the organic rich or coal bands are cemented, heavily fractured or folded and contain pyrite. These sections are alternated by fine sandstone, frequently showing subparallel or crosscutting wavy layering.

2.5 Solling Fat Sandstone member (RNSOF)

For well L09-10 core slabs are available over the depth interval between 3140-3244 m, comprising the basal half of the Solling Fat Sandstone member of the Upper Germanic Triassic Group. The litho-stratigraphic unit consist of very well to moderately sorted sandstone with intercalations of very thin, reworked layers or flasers of compact claystone. The unit is predominated by sandstone, showing fine (sub)parallel layering of fine grained sand with occasional layers of coarser, poorly sorted (breccia) grains up to a meter in thickness. The sandstone units show cementation with salt in cm-thick bands and with hematite in dark red to pale green bands up to a few meters thick. Hematite cementation and the presence of (very) coarse grained layers are especially common and dominant in the lower part of the drilling core.

2.6 Lower Volpriehausen Sandstone Member (RBMVL)

Part of the Volpriehausen Formation is cored in well M07-02 over depths between 2800-2810 m, corresponding to part of the Lower Volpriehausen Sandstone Member of the Lower Germanic Triassic Group. Its lithology is marked by parallel layered, moderately to well sorted medium grained sandstone. Locally the sandstone is cemented by calcareous material. Isolated occurrences of coarser bands are recorded on a few levels. Towards the basal part of the cored interval, the grain size decreases and the lithology shifts to silt or claystone.

2.7 Lower Slochteren Sandstone Member (ROSLL)

The upper 8 meters of the drilling core specimen of well G18-01 (3822-3894 m) show the expression of the Lower Slochteren Sandstone Member of the Upper Rotliegend Group. This unit is characterized by medium to fine grained, laminated sandstone, with coarser grained, badly sorted layers and clay-filled burrows.

3 Calculation method

Accurate estimates on porosity values in certain stratigraphical intervals can be derived from several well log types, i.e. the sonic, neutron or bulk density log. As the purpose of this study is to produce porosity estimates from well logs that generally lack core-measured porosity values, theoretical methods of calculation are preferred over empirical relationships between the well log signal and available porosity measurement data from drilling cores. Theoretically based calculations are less influenced by local conditions and therefore more widely applicable. Theoretical relationships between porosity and respectively neutron, sonic and bulk density logs are evaluated below (after Rider, 1986).

3.1 Neutron log

The relation between porosity and neutron log is not very straightforward. A linear relationship only exists for limestone lithologies. The general mathematical expression is as follows:

$$\log_{10} \phi_N = aN + B \qquad (1)$$

where ϕ_N = porosity
N = neutron tool reading
a, B = constants

There exist no theoretical or proven values for the constants a and B in formula (1), which implies that empirical correlation to measured core values will be needed to enable neutron log derived porosity calculations. This seriously reduces the compatibility of this approach to multiple well logs and litho-stratigraphic intervals. Moreover, interpretation of the log signal inhibits uncertainty, as the neutron logging tool records the hydrogen index of the lithology. This index can be high both in porous sandstones due to the present pore fluid as well as in hardly porous shales as a result of water within the molecule structure or adsorbed between mineral layers. Therefore, in some cases the neutron log shows hardly any correlation to measured porosity values.

3.2 Sonic log

Porosity can be calculated from sonic logs using the Wyllie equation:

$$\phi_S = \frac{\Delta t - \Delta t_{ma}}{\Delta t_f - \Delta t_{ma}} \qquad (2)$$

where ϕ_S = porosity
Δt = tool measured interval transit time
Δt_{ma} = transit time of matrix material
Δt_f = transit time of interstitial fluid

Table 2. Sonic log response values for matrix material. From: Rider (1986).

	Material	Sonic transit time (μs/ft)
Common lithologies	Sandstones	53-100
	Limestones	47.6-53
	Shales	60-170
Fluids/Gas	Methane	626
	Oil (40° API)	238
	Water (80° F)	
	pure	189-207
	salt (33,000 ppm)	180

In general porosities derived from the sonic log are inferior to neutron or density log calculated porosities (Rider, 1986). In order to calculate porosity from the sonic log signal, specific information on the matrix material and fluid transit times for the investigated litho-stratigraphic units is required. Unfortunately such data is not available and representing values need to be gathered from literature (table 2). Although transit times for known matrix material or pore fluid can be fairly constrained, uncertainty rapidly increases with lithological or hydrochemical variation (e.g. Rider, 1986). As a consequence comparison to measured values shows reasonable calculated porosity values, although generally not as precise as those derived from bulk density logs. However, this approach at least gives the order of magnitude of porosities and if bulk density logs are absent, the sonic log may be used as an alternative for porosity estimation.

3.3 Bulk density log

The relationship between bulk density logs and porosity is similar to the Wyllie equation:

$$\phi_D = \frac{\rho_{ma} - \rho_b}{\rho_{ma} - \rho_f} \tag{3}$$

where ϕ_D = porosity
ρ_b = tool measured bulk density
ρ_{ma} = matrix (or grain) density
ρ_f = fluid density

Determination of porosity values from bulk density logs provides better estimates, as it enables twofold incorporation of measured values on cored intervals. Over these intervals data is available not only on true porosities, but also grain density is directly measured on core samples. Moreover, the remaining variable (i.e. fluid density) can be deduced from other available parameters, as will be discussed later. Therefore this method provides better constraints relative to other approaches. Calculations based on sonic or neutron logs would only benefit from calibration to measured porosities, while the formula input would be derived from literature values.

4 Application of the bulk density log

Based on the discussion above, the bulk density log is considered to be the most reliable method of porosity calculation from well logs in this case. Advantages over the other methods are:

- the existence of a clear and linear theoretical relationship between bulk density and porosity;
- the availability of high resolution data on matrix densities for cored intervals in many litho-stratigraphic units of multiple wells;
- the possibility to evaluate fluid density values directly from resistivity measurements.

For some specific wells, however, calculated porosities derived from other log types or combinations of these with density log results showed higher correlation to measured values. As the method is intended to be widely applicable, bulk density log based calculations are favoured nonetheless. The resulting porosities are subsequently compared to available porosity measurement data from core plugs.

In general the bulk density log is accompanied by the density correction log (DRHO), which records absolute deviations of the log signal. If this deviation exceeds 0.15 or -0.15 g/cm^3, the bulk density log signal is no longer trusted and measurements on these intervals are ignored (Ramaekers, 2006). Along some intervals of interest, the bulk density log is not available at all and as a result no porosity calculations could be performed using the method described here.

The bulk density log, as any other type of log, records its signal over a short depth interval as it moves through the borehole. These recordings consequently produce a slightly smoothed log curve of readings. However, the intervals allow comparison to plug measurements (i.e. point sources) as they are sufficiently small. Moreover, the final calculated porosity values are averaged over much larger intervals of litho-stratigraphic units and represent a rough indication of porosity over these units. Also note that the porosity measurements are performed at atmospheric pressure and would need in-situ correction to be comparable to true porosity at depth or calculated values from logs.

5 Impact of shale

The evaluated potential Triassic and Jurassic reservoir levels of the Dutch offshore domain predominantly consist of sand-shale sequences. Above relationships between porosity and either transit time or bulk density (formulas (2) and (3)) take into account single values for the matrix parameters (i.e. grain density and matrix transit time, respectively). As long as these parameters remain constant along the borehole the relationship between the log values and porosity can be very close. If, in contrast, the matrix properties vary over the investigated depth interval, the porosity calculated using formula (2) or (3) is not correct. If properties for quartz would be applied, calculations in sand-shale sequences therefore should be compensated for the shale fraction. In this case the relative amount of shale present in the rocks needs to be evaluated.

Theoretically, the volume fraction of shale can be derived from the gamma ray log as the shale volume is linearly proportional to the gamma ray log value (*GR*). Note that this is valid only under the assumption that radioactive potassium elements of the shale minerals are the sole contributors to the gamma ray log signal:

$$V_{sh} = \frac{GR - GR_{\min}}{GR_{\max} - GR_{\min}} \qquad (4)$$

where V_{sh} = relative volume of shale

Formula (4) would result in good estimates on the volumetric shale fraction only if the maximum and minimum gamma ray log values correspond to clean sandstone ($V_{sh} = 0\%$) and pure shale ($V_{sh} = 100\%$), respectively. However, the relationship will become oblique in all other cases. It is therefore highly unlikely that such analysis will return reliable shale volumes for different wells and litho-stratigraphic units. Uncertainty increases considering the fact that gamma ray log values vary enormously between wells and would need to be calibrated for every single well. Still the gamma ray log can be successfully applied in the more qualitatively operation of determining the net-to-gross ratio. To this purpose the potential reservoir intervals are divided into pay and no-pay zones based on the gamma ray log signal, relative to the 0.5 level of V_{sh} calculated from formula (4). Although this is a rather rough approach, it is valuable nonetheless.

Alternatively, the presence of shale can be deduced from the combined bulk density and neutron logs. The procedure depends on the fact that both logs essentially display the same parameter, i.e. porosity. Theoretically it should therefore be possible to superimpose the logs according to the relationships shown in table 3.

Table 3. Linear theoretical relationship between porosity, neutron log signal and bulk density for clean, fresh water-filled (density 1.0 g/cm^3) limestone

Porosity (%)	Neutron log signal	Bulk density (g/cm^3)
0	0.0	2.7
100	1.0	1.0

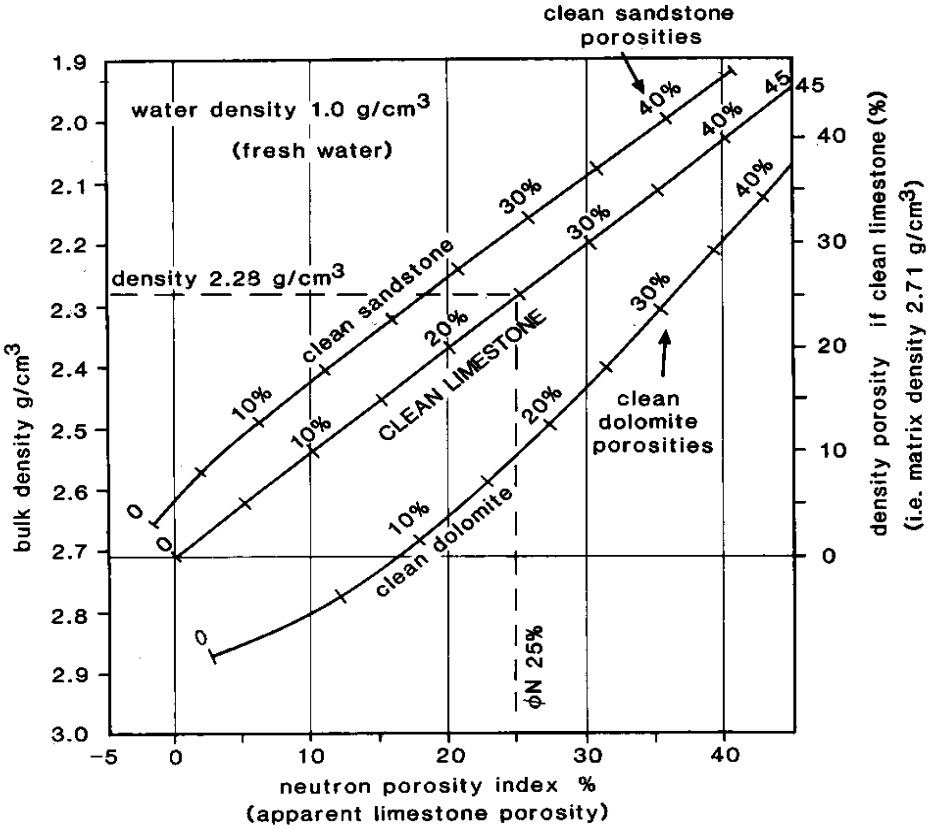

Figure 2. Bulk density–neutron cross plot showing the differing effect of matrix type on both logs. From: Rider (1986)

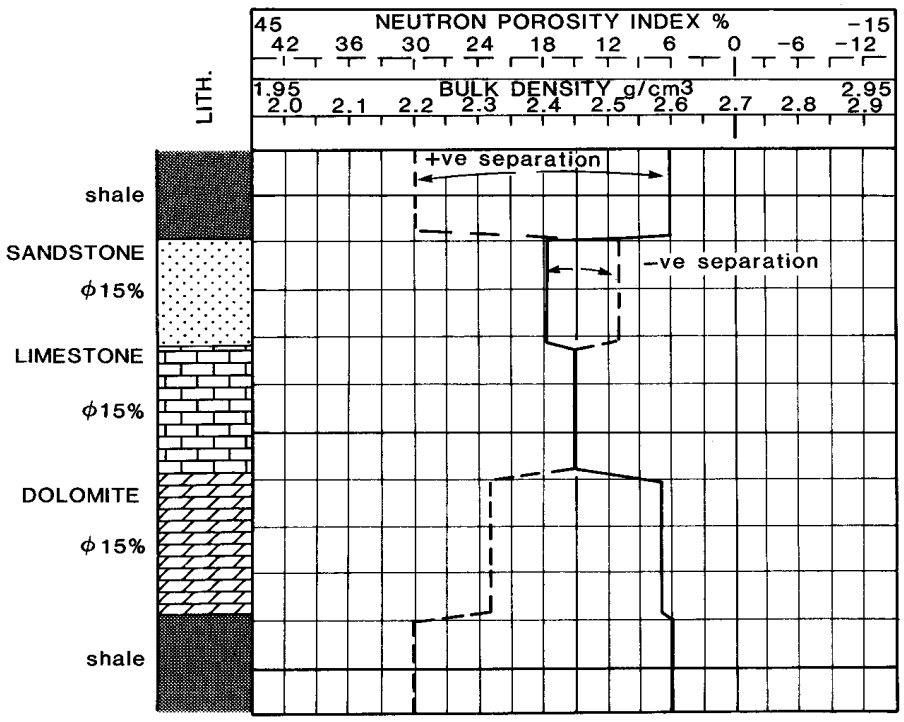

Figure 3. Idealized neutron-density log combination responses for different lithologies (all with 15% water-filled porosity), showing characteristic separation. From: Rider (1986)

In practice however, this is true only for clean, water-filled limestones. For other matrix materials the relationship between bulk density and neutron log value is not exactly equal (figure 2). The resulting separation between the bulk density and neutron log curves plotted on compatible scales is diagnostic for certain lithologies, such as limestone, dolomite, sandstone and shale (figure 3). Furthermore, it is considered to be roughly linearly related to the volume of shale in a sand-shale system (Rider, 1986).
This method is fundamentally more reliable than using the gamma ray log (Rider, 1986), but its application is hampered by factors that influence bulk density or neutron log signals (e.g. cementation, presence of heavy minerals, presence of gas). Qualitative application of this method at least results in a subdivision of potential reservoir intervals into pay and no-pay zones comparable to that based on the gamma-ray log.

As described here, the classification of lithologies in pay and no-pay zones can be executed through two independent methods. Both result in comparable subdivisions. Unlike the application of bulk density and neutron logs, the gamma ray log signal in sand-shale sequences is predominantly influenced by the presence of potassium-bearing clay minerals in shales. Therefore this approach is more directly linked to the occurrence of shale and used in determining the net-to-gross ratio.
The recorded minimum and maximum log values are evaluated for the individual wells over potential reservoir intervals of the Upper Jurassic Schieland and Scruff Groups, the Lower Triassic Main Buntsandstein Subgroup, the Upper Rotliegend Group and the Solling Fat Sandstone member of the Upper Germanic Triassic Group. The extreme values are subsequently used in formula (4) to determine the relative volumetric shale content. Shale content below 0.5 is regarded as net or pay zones, while higher values represent the remaining no-pay intervals.

The correction for the volume of shale could be applied in formula (3) as follows:

$$\phi_D^{V_{sh}} = \frac{\rho_{ma} - \rho_b}{\rho_{ma} - \rho_f} - V_{sh} \cdot \frac{\rho_{ma} - \rho_{sh}}{\rho_{ma} - \rho_f} \qquad (5)$$

where $\phi_D^{V_{sh}}$ = porosity compensated for presence of shale
ρ_{sh} = shale density

Using this formula would impose new uncertainties, as the shale properties are not as much constrained as the grain density and transit time of other common lithologies. Related to the amount of compaction shale densities roughly vary between 1.8-2.75 g/cm^3 (Rider, 1986). Moreover, measured matrix densities from core plugs represent matrix material consisting of both sand (quartz) grains and shale particles. This prohibits straightforward application of formula (5) as it distinguishes a quartz-matrix density and separate shale density.

6 Determination of matrix density

Formula (3) requires input of values for matrix density and fluid density. Literature values for matrix densities roughly range from 1.8 to 2.75 g/cm^3. However, more specific information is available for specific litho-stratigraphic units through plug sample measurements. This data is digitized and represented per unit in histograms, showing reasonably well, normally distributed populations (figure 4). As measured values on specific litho-stratigraphic units of different wells (i.e. different locations) are combined and the distributions in figure 4 are reasonably narrow, matrix densities for single units seem to show little vertical and lateral variation. Therefore, it seems legitimate to calculate mean values and standard deviations to represent the sampled units in all wells. Unfortunately, direct measurements on matrix density are not available for all litho-stratigraphic units at interest. In order to quantify this property for other units, the averaged values of comparable lithologies at similar stratigraphic levels are used.

The average matrix density value of Terschelling Sandstone Member (SLCTS) is applied on the unit itself as well as on the lithologically resembling units of the Terschelling Formation (SLCT), i.e. the Terschelling Argillaceous Member (SLCTA) and the Terschelling Arenaceous Member (SLCTB). Matrix densities for the other sandstone lithologies in the Scruff Greensand Formation (SLSG), i.e. the Stortemelk Member (SLSGS), are based on the average of the measured values for the Scruff Spiculite Member (SLSGP). For the Oysterground Member (SLCTO) limited, but high-precision measurements are available and used to describe this unit. The remaining units of the Friese Front Formation (SLCF), among which the Rifgronden Member (SLCFR), are represented by the average value of combined measurements on these units.

Table 4. Matrix density derived from measurement distributions for specific litho-stratigraphic units.

Litho-stratigraphic unit		Mean matrix density [g/cm^3]	Standard deviation [g/cm^3]
Schill Grund Formation	SLSS	2.710	0.016
Scruff Greensand Formation [1]	SLSG	2.634	0.026
Terschelling Formation (except SLCTO) [2]	SLCT	2.692	0.063
Oysterground Member	SLCTO	2.651	0.010
Friese Front Formation	SLCF	2.652	0.097
Solling Fat Sandstone member	RNSOF	2.540 [5]	- [5]
Detfurth Clay Member [3]	RBMDC	2.720	0.042
Lower Detfurth Sandstone Member	RBMDL	2.698	0.038
Volpriehausen Clay-Siltstone Member	RBMVC	2.720	0.042
Lower Volpriehausen Sandstone Member	RBMVL	2.645	0.040
Rogenstein Member	RBSHR	2.749	0.026
Ten Boer Member [4]	ROCLT	2.705	0.069
Upper Slochteren Member	ROSLU	2.705	0.069
Ameland Member [4]	ROCLA	2.705	0.069
Lower Slochteren Sandstone Member	ROSLL	2.682	0.014

[1] *Parameters derived from measurements on Scruff Spiculite Member (SLSGP)*

[2] *Parameters for sandstone units in SLCT derived from measurements on Terschelling Sandstone Member (SLCTS)*

[3] *Parameters derived from measurements on Volpriehausen Clay-Siltstone Member (RBMVC)*

[4] *Parameters derived from measurements on Upper Slochteren Member*

[5] *Applied mean matrix density determined based on best correlation (see text)*

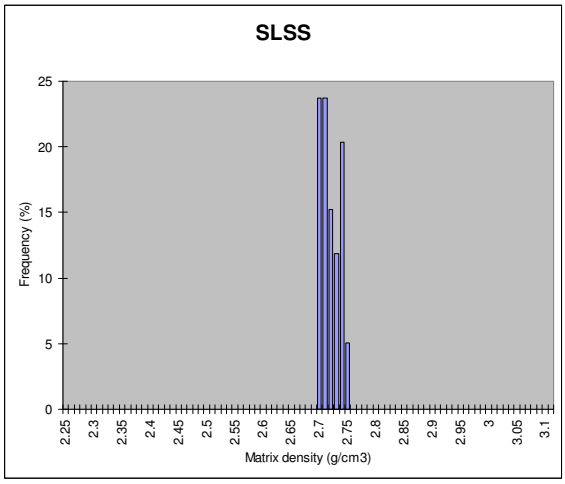

2.710 ± 0.016 g/cm^3, N = 59

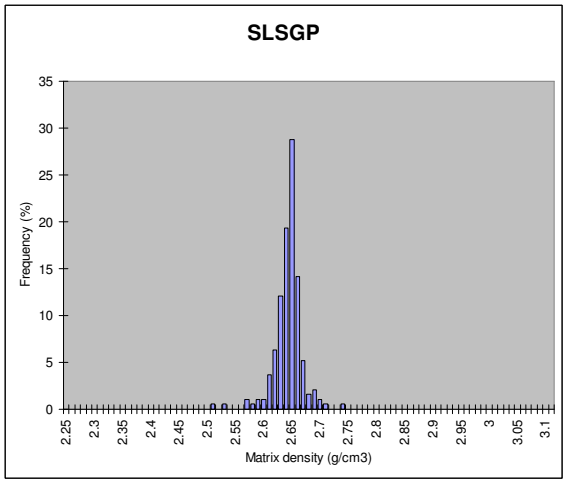

2.634 ± 0.026 g/cm^3, N = 191

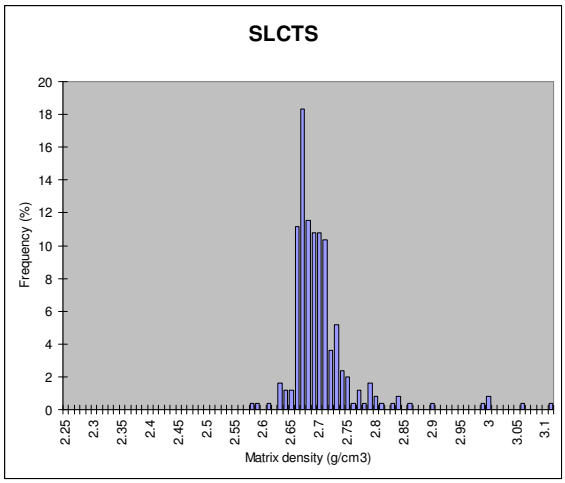

2.692 ± 0.063 g/cm^3, N = 251

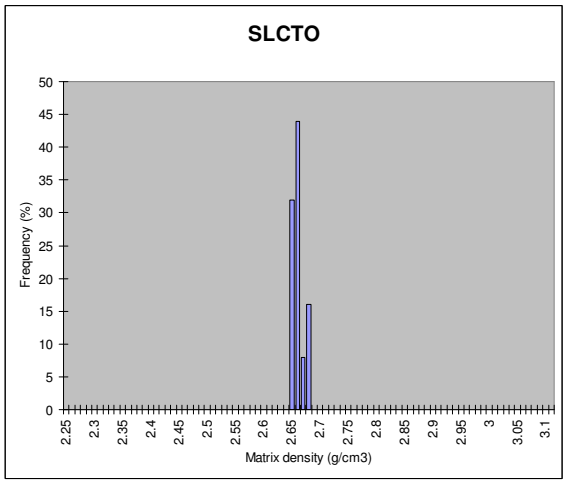

2.651 ± 0.010 g/cm^3, N = 25

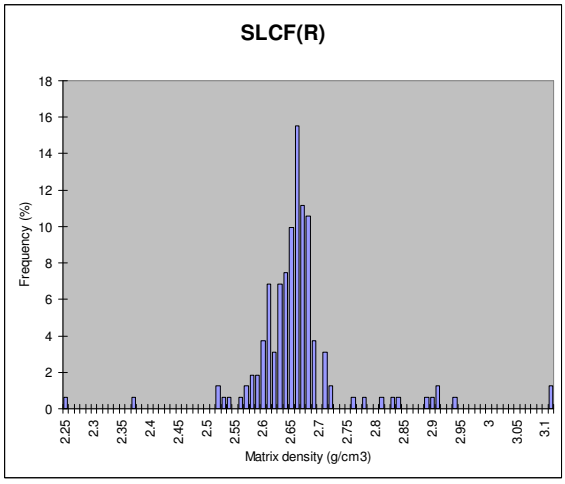

2.652 ± 0.097 g/cm^3, N = 161

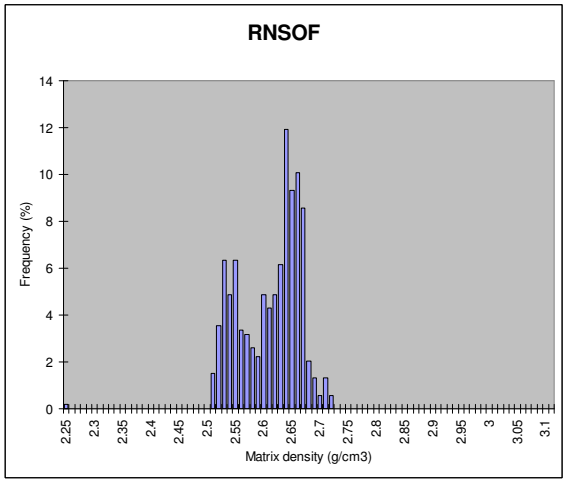

2.602 ± 0.057 g/cm^3, N = 536

Figure 4. Matrix density distributions for litho-stratigraphic units (SLSS, SLSGP, SLCTS, SLCTO, SLCF(R), RNSOF), stating calculated mean value, standard deviation and population per unit.

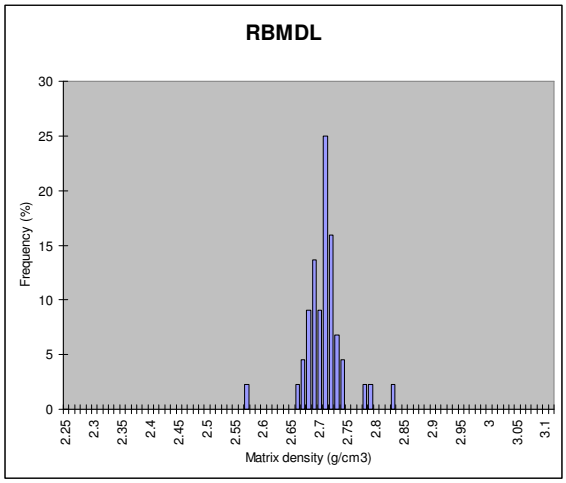

2.698 ± 0.038 g/cm^3, N = 44

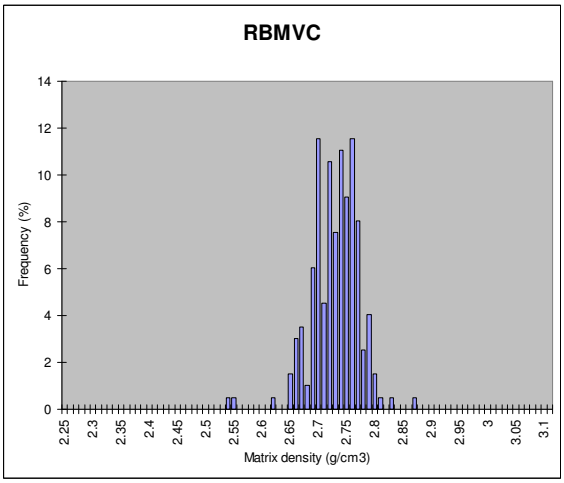

2.720 ± 0.042 g/cm^3, N = 199

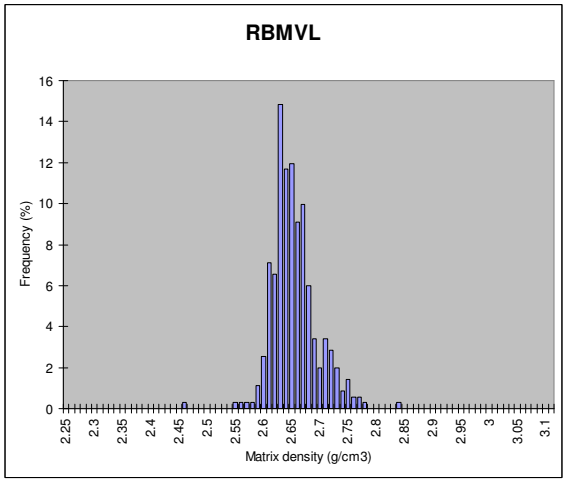

2.645 ± 0.040 g/cm^3, N = 351

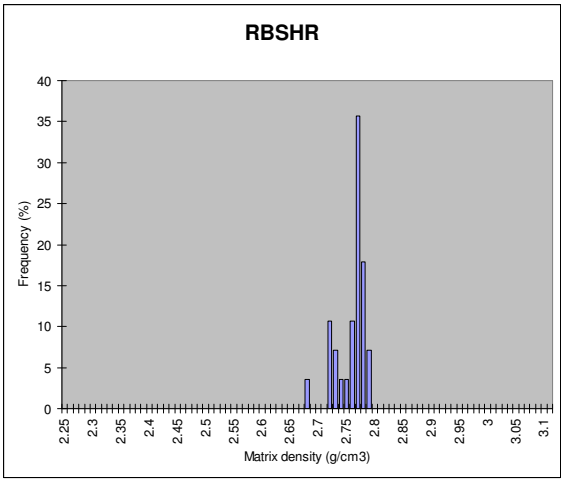

2.749 ± 0.026 g/cm^3, N = 28

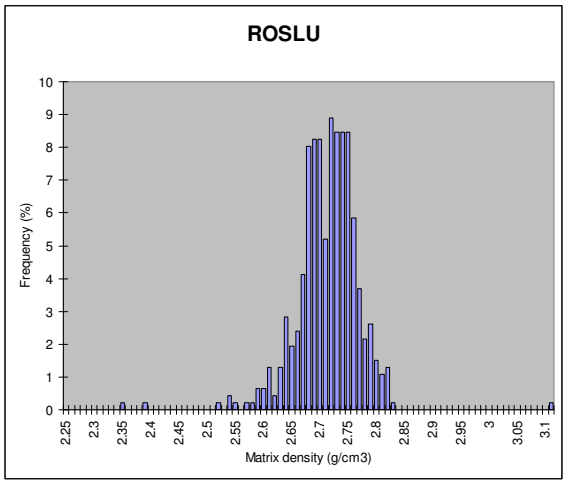

2.705 ± 0.069 g/cm^3, N = 461

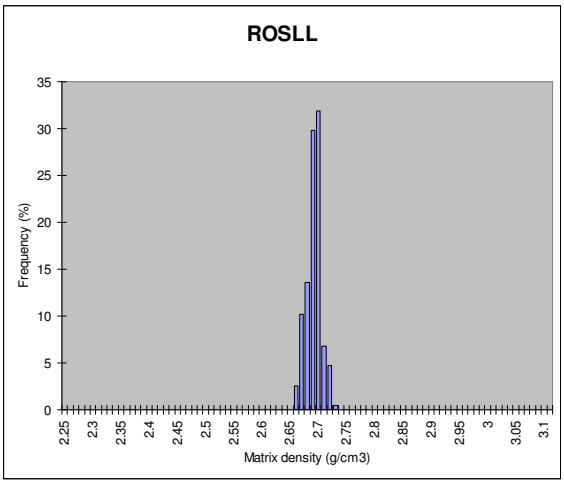

2.682 ± 0.014 g/cm^3, N = 235

Figure 4 (continued). Matrix density distributions for litho-stratigraphic units (RBMDL, RBMVC, RBMVL, RBSHR, ROSLU, ROSLL), stating calculated mean value, standard deviation and population per unit.

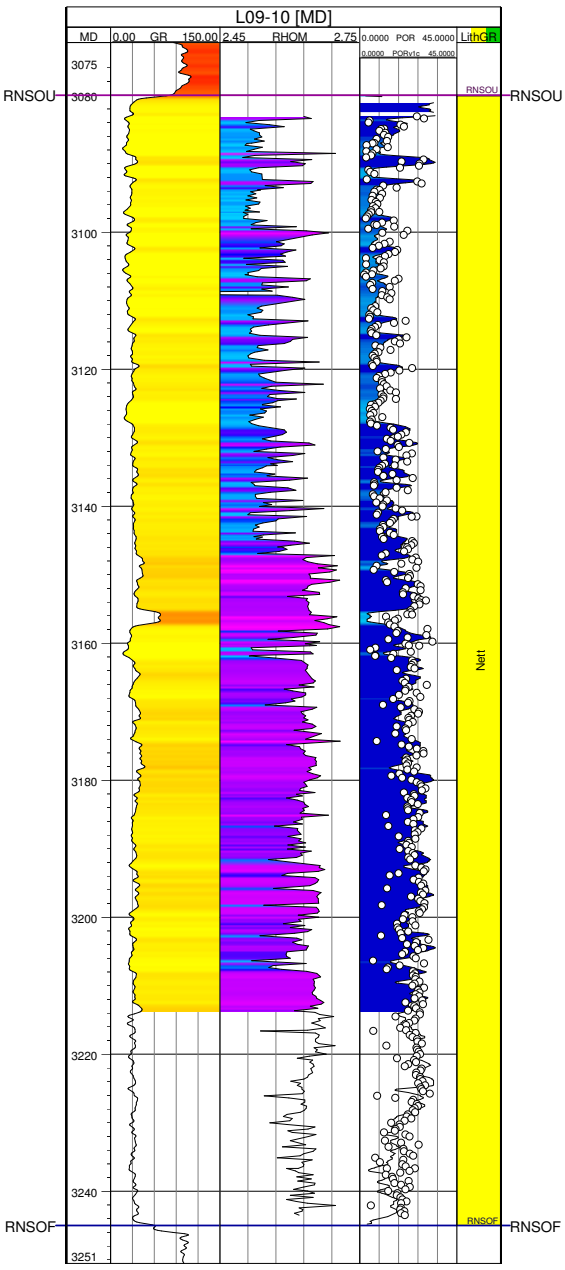

Figure 5. Matrix density variation in Solling Fat Sandstone member (RNSOF) of L09-10 well (second column); gamma ray log in first column; measured and calculated porosity (dots and lines, respectively) in third column.

For the Oysterground Member (SLCTO) limited, but high-precision measurements are available and used to describe this unit. The remaining units of the Friese Front Formation (SLCF), among which the Rifgronden Member (SLCFR), are represented by the average value of combined measurements on these units.

Since the measured Solling Sandstone member (RNSOF) matrix density shows a distinct bimodal distribution, calculating and applying a mean value would not represent the entire unit well. In this case measurements were available from a single well (i.e. L09-10). Figure 5 indicates that in this well the upper part of the unit consists of matrix material with a lower density, averaged at about 2.54 g/cm^3, with respect to that of the lower section, showing higher matrix densities around 2.64 g/cm^3. Because application of the lower mean matrix density of the upper part resulted in a very good porosity estimation of the entire unit (figure 5), this density is applied for the Solling Fat Sandstone member in all investigated wells.

The matrix density used for the Detfurth Clay Member (RBMDC) is derived from the Volpriehausen Clay-Siltstone Member (RBMVC), while the Ten Boer (ROCLT) and Ameland Member (ROCLA) of the Upper Rotliegend Group, that occasionally contain sandy layers, are assigned the Upper Slochteren Member (ROSLU) density. The distribution of the latter matrix density also shows some bimodality (figure 4). However, since the separation between both peaks is small, the average value of the total population is used here. The applied matrix densities for all litho-stratigraphic units are listed in table 4.

7 Determination of pore fluid density

The bulk density logging tool investigation depth generally is limited to about 10 cm (Rider, 1986). Therefore, the tool mainly records the invaded zone where the aqueous drilling mud filtrate replaced formation water or oil. As a consequence especially in porous zones the fluid density involved in formula (3) represents the mud filtrate density, rather than the original pore fluid density. This property can be quantified using its salinity, which in turn can be derived from the mud filtrate resistivity, corrected for temperature (Ramaekers, 2006).

Data on resistivity and borehole temperature measurements is available from the drilling report and log header for NAM-drilled wells only. For these wells the mud filtrate salinity and density is calculated by Ramaekers (2006) using the ELAN calculator. For other wells the average of recorded mud filtrate densities (1.0788 g/cm^3) has been taken (table 5). This is regarded to be legitimate as differences between calculated results are fairly small and even the mud filtrate density is roughly comparable to that of formation water or oil. Moreover, error propagation is limited as the fluid density in formula (3) is subtracted from the much higher matrix density in the denominator, the result being significantly larger than the numerator. The maximum propagation error in the resulting porosity as a consequence is very small.

Table 5. Applied mud filtrate density for all evaluated wells

Calculated from resistivity data		*Average value applied* [1]			
Well ID	Mud filtrate density (g/cm^3)	Well ID	Mud filtrate density (g/cm^3)	Well ID	Mud filtrate density (g/cm^3)
G16-01	1.1711	F15-02	1.0788	L06-02	1.0788
L02-02	1.0725	F17-01	1.0788	L07-04	1.0788
L02-05	1.0617	F17-04	1.0788	L08-02	1.0788
L02-07	1.0573	F18-01	1.0788	L08-03	1.0788
L05-01	1.0001	F18-02	1.0788	L09-10	1.0788
L05-04	1.1682	F18-09	1.0788	L12-03	1.0788
L06-01	1.1519	G17-01	1.0788	L12-05	1.0788
L06-03	1.1108	G18-01	1.0788	M03-01	1.0788
L12-02	1.0469	L01-06	1.0788	M04-01	1.0788
L15-01	1.1008	L02-04	1.0788	M07-01	1.0788
M01-01	1.1504	L03-01	1.0788	M07-02	1.0788
M01-02	1.0042	L03-02	1.0788	M09-01	1.0788
M08-01	1.0839	L03-04	1.0788	M10-02	1.0788
M11-01	1.0370	L04-03	1.0788	M10-04	1.0788
mean value	1.0788				

[1] *Wells of which no specific data is available are assigned the mean mud filtrate density value calculated from available data, i.e. 1.0788 g/cm^3.*

The mean value agrees with values obtained through other methods: from drilling reports the basal drilling fluid density is recorded. This may well be indicative for the mud filtrate density as the basal fluid is in many aspects similar to the filtrate, i.e. the mud suspension. As many wells penetrate the evaporite-rich Zechstein Group, the drilling fluid is expected to be based on salt water. In more than 30 wells initial mud densities are registered between 1.02-1.16 g/cm^3 with a mean value of 1.081 g/cm^3. This is comparable to the value of 1.0788 g/cm^3 calculated from resistivity values.

One of the parameters involved in this evaluation is the measured borehole temperature. Single values of this temperature are assigned to recorded depth intervals. Plotting these values for available wells against mean depth of the potential reservoirs concerned results in a graph showing a rough thermal gradient averaged over several locations of the Terschelling Basin and southern Central North Sea Graben area (figure 6). The gradient is mathematically described by formula (6):

$$T(z) = 0.033952 \cdot z + 11.39 \qquad (6)$$

where T = temperature in ºC

z = depth in meters

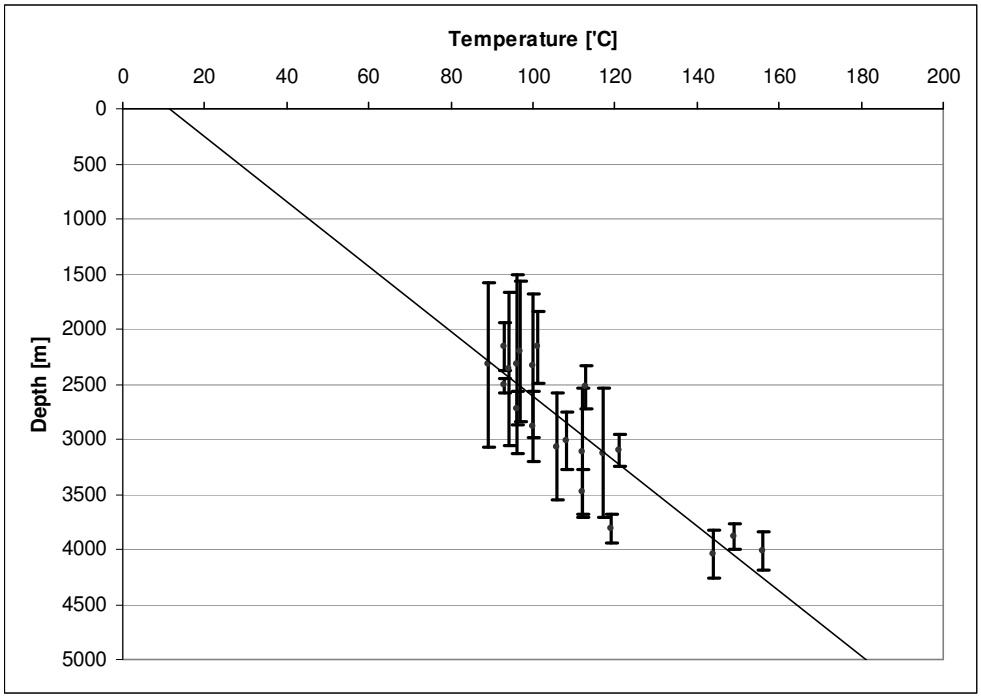

Figure 6. Thermal gradient of the Terschelling Basin and southern Central North Sea Graben region from borehole temperatures of NAM-drilled wells. Correlation coefficient of temperature and depth is 0.7775. Bars indicate depth interval of potential reservoir unit.

8 Gas-bearing reservoirs

As pointed out before, the bulk density logging tool predominantly measures the invaded zone alongside the borehole. For water or oil-bearing formations the invaded zone is mainly filled with penetrated mud filtrate. Gas-bearing reservoirs in contrast present a more complex situation. The presence of gas in the pore space complicates the approach described above. As a result of the high mobility of the gas phase, the invading mud filtrate is rapidly replaced by the gas again. The bulk density logging tool therefore records a significantly lower value as the gas density is negligible compared to the applied pore fluid density. As a consequence, calculating porosity from the bulk density log in gas-bearing zones would result in highly overestimated values. In contrast the neutron log derived porosity would be underestimated if gas is present in the pore spaces, as the recorded hydrogen index of gas is much lower than that of water or oil. Therefore, in order to correct for this gas-effect commonly the arithmetic mean value of the bulk density log derived density and the neutron log derived density is used (Rider, 1986):

$$\phi = \frac{\phi_{NPHI} + \phi_{RHOB}}{2} \tag{7}$$

where ϕ = porosity
ϕ_{NPHI} = porosity derived from neutron log
ϕ_{RHOB} = porosity derived from bulk density log

However, as mentioned before, the neutron log cannot be used directly to calculate porosities in sequences other than limestone lithologies as the log returns porosity values equivalent to fresh water-filled, clean limestone values (figure 2):

$$\phi_{NPHI}^{L} \triangleq \frac{\rho_L - \rho_b}{\rho_L - \rho_w} \tag{8}$$

where ϕ_{NPHI}^{L} = limestone equivalent porosity
ρ_b = tool measured bulk density
ρ_L = limestone matrix density (2.70 g/cm^3)
ρ_w = fresh water density (1.00 g/cm^3)

For different types of lithology and pore fluid the porosity can be calculated from the neutron log signal using:

$$\phi_{NPHI} = \frac{\rho_{ma} - \rho_L + \phi_{NPHI}^{L} \cdot (\rho_L - \rho_w)}{\rho_{ma} - \rho_f} \tag{9}$$

Information on the presence of gas in litho-stratigraphic units in the investigated area is gained from TNO's DINO borehole database and refined when possible using well log information (values for the bulk density and neutron logs both abruptly decrease when gas is present). Formulas (7) and (9) are applied for gas-bearing litho-stratigraphic intervals using the limestone and fresh water density

values stated above. The matrix and fluid density are derived per unit according to the method described above. Known gas-bearing zones are generally densely sampled and measured. As a result specifically in these intervals a lot of information on true porosity is available. Comparison of resulting to measured values show very good correlations.

The Solling Fat Sandstone member (RNSOF) of the L09-10 well is an exception to this description. For this interval also abundant porosity measurements are available, but non-gas-corrected calculated porosity values correspond much better to these measurements than gas-corrected values do. Therefore, no gas correction is applied on this specific interval. For the Lower Volpriehausen Sandstone Member (RBMVL) of well L02-07 no gas-correction has been applied as well, as no neutron log is available on that interval (table 6). The Schieland Group interval of the same well is recorded to bear gas as well. However, since neutron log values are extremely high (up to 0.53 limestone porosity units) no neutron log gas correction is implemented, as the resulting value from formula (7) would further overestimate the porosity.

Another manner to correct for the presence of gas could be by simply using the gas density value (i.e. near zero) for the pore fluid density in formula (3). However, in practice gas will generally not be present in the total pore volume of the specific units, but rather in the top section only. Therefore using this less complicated approach would require to exactly specify the intervals that contain pore gas as all values calculated in this way are affected by the correction. In contrast, this is less of a problem when employing the mean value of bulk density and neutron log for gas corrections. Inappropriate application of this adjustment in non-gas-bearing zones is allowed as the recalculated neutron log value (see formula (9)) closely resembles porosity values calculated using the bulk density log as described before.

Table 6. Recorded presence of gas in litho-stratigraphical units

Well ID	Litho-stratigraphical unit	Top [m]	Bottom [m]
L02-05	RBMVL	4161.0	4200.0
L02-07 [1]	RBMVL	4030.0	4071.0
L04-03	ROSLL	3697.0	3776.0
L06-02	SLCTS	2463.0	2500.0
L09-10 [2]	RNSOF	3080.0	3245.0
L12-02	ROSLU	3034.0	3135.0
L12-03 [3]	ROSLU	2912.0	2996.0
L12-05	ROSLL	3430.0	3438.0
L15-01	ROSLU	2865.0	2989.0
M01-02	RBMVL	3917.0	3944.0
M11-01	ROSLU	2789.0	2910.0

[1] *no gas correction applied over this interval (no neutron log available)*

[2] *no gas correction applied over this interval (uncorrected values much better correlated to measurements)*

[3] *no porosity calculated as no bulk density log is available over this interval*

9 Porosity calculation

In order to calculate porosity values for the potential reservoir units of the Jurassic and Triassic of the Dutch offshore NCP-2A region, the methods described above are applied to available well data. The entire process is schematized in figure 7. To this purpose automated routines were developed and applied in Microsoft Excel that required input parameters bulk density and neutron log values as a function of depth for every evaluated well. Furthermore, the litho-stratigraphic boundary depths of the specific potential reservoir units for all wells were needed as well as the data on matrix and mud filtrate density derived from the methods described above. The calculated porosity 'log' curves were imported into Petrel, where they are combined to the net-gross divisions derived from the gamma ray log, resulting in porosity distributions over net (i.e. potential reservoir) intervals (Appendix I). These distributions are subsequently imported in Excel to calculate mean values and standard deviation for the pay zones of potential reservoir units (Appendix II). Note that the calculated standard deviation describes the width of the distribution of calculated porosity values over specific depth intervals, rather than quantifying the error in calculating porosity form well logs.

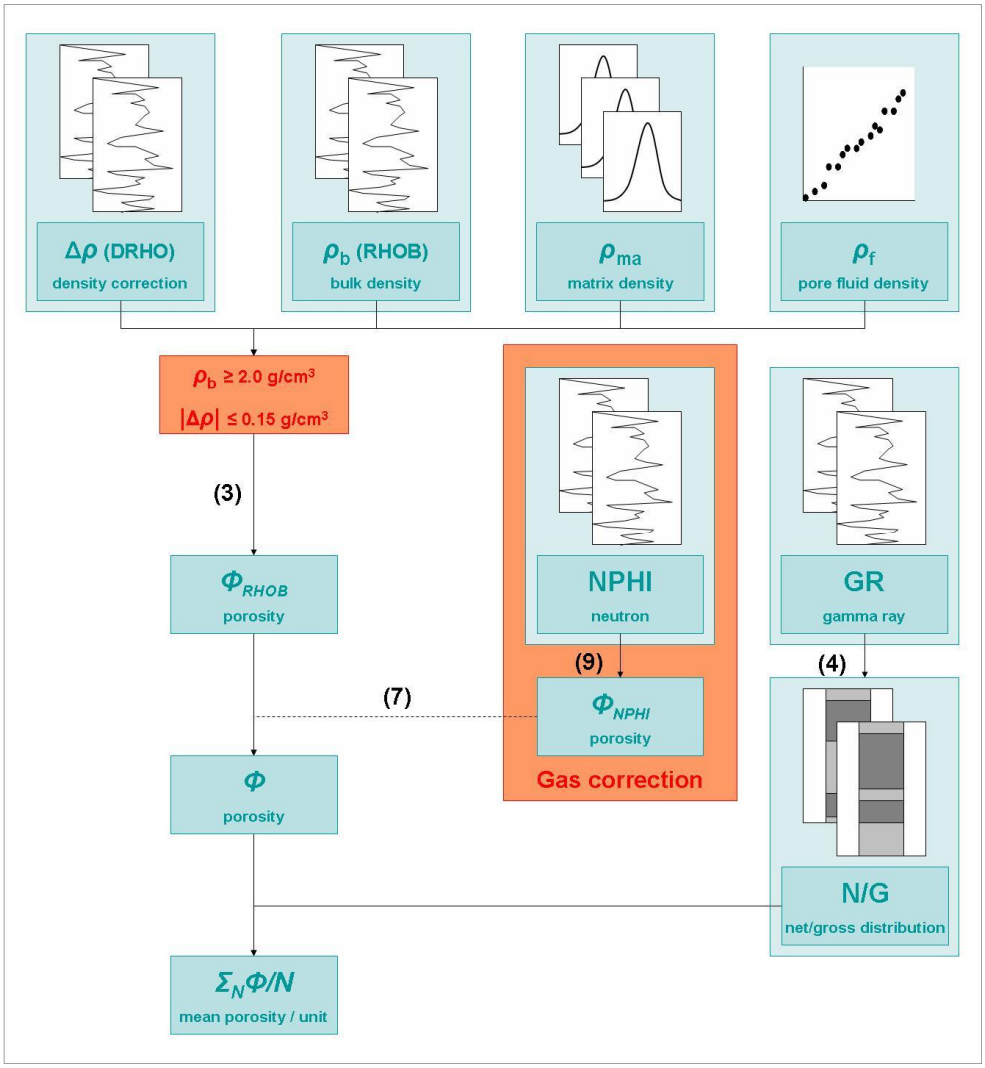

Figure 7. Schematic reflection of porosity calculation from well logs. Indicated numbers refer to formulas applied in calculation steps. In red specific conditions are represented.

Table 7. Applied shift in log curves based on correlation between porosity measurements and calculations.

Well ID	Shift[1] (m)
F15-02	+2.15
F17-04	-1.95
F18-09	+2.69
L02-02	+2.56
L03-01	+3.42
L05-01	+5.55
L06-02	+3.00
L06-03	+0.50
L07-04	+5.90
L12-02	+2.66
L15-01	+4.84
M01-02	+1.80
M07-02	+1.20
M08-01	+3.80
M10-02	+2.20
M10-04	+1.30

[1] *positive numbers indicate downward shift; negative numbers indicate upward shift*

Subsequently, the resulting porosity logs are compared to measured values. The fact that measured depth values of the logs are not always perfectly coinciding with measured depths used for measurements is an obstacle. Due to the weight of the logging tool and cable itself, the cable is strained a little and therefore the log data can be appointed to too shallow levels with separations up to a few meters. Correction of data for this effect is not always performed adequately. However, if the relationship between the measured porosities and log signals is very obvious, which is the case especially in alternating sand-shale sequences, the logs can be legitimately shifted within a few meters (table 7). Evaluated drilling reports support downward shifts in this range. However, if the relation between measurements and log signals is unclear or the vertical interval and/or continuity of measurements is not sufficiently large, shifting the log curves cannot be justified. The unexpected upward shift of the F17-04 log will not be discussed here, but is legitimated as shown through the log-calculated porosity (figure 8). It is important to note that shifting logs has no effects on the porosity calculations and is solely intended to compare calculated data to measurements.

The presence of (reworked) coal or organic matter-rich material in the Friese Front Formation (SLCF) and Oysterground Member (SLCTO) shows a negative effect on the reliability of porosity calculations using the bulk density log: as coal density is much lower than densities of other matrix material, the bulk density shows lower values. In turn using formula (3) this results in high, overestimated calculated porosities (figure 9). To practical deal with this situation, bulk density values below 2.0 g/cm^3 are not processed in the Schieland Group and the Scruff Group. Manually bulk density log readings below 2.2 g/cm^3 are ignored for the Friese Front Formation and Oysterground Member only. Of course it may be possible that some genuine sand-shale porosity information is neglected this way, as loose sand and clay can show bulk densities of 2.0 g/cm^3.

This approach is supported however by calliper logs that show high peaks at levels coinciding with extremely low bulk density value peaks. Especially since the bulk density tool has a very small investigation depth and therefore is very susceptible to borehole conditions, calliper deviations point to inaccuracy in the bulk density signal.

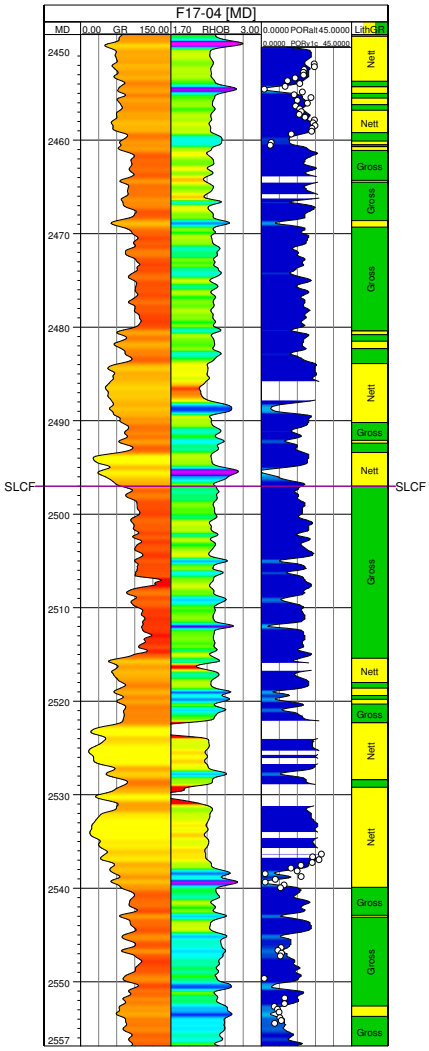

Figure 8. Very good fit of measured porosity (white dots) to calculated values (in blue) after curve shift of -1.95 in well F17-04. First column: gamma ray log; second column: bulk density log; fourth column: nett-gross.

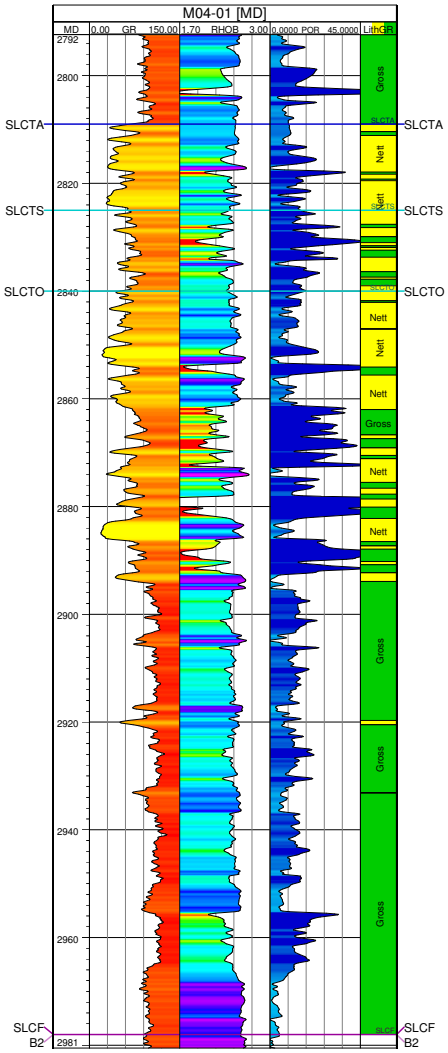

Figure 9. Extremely low bulk density values in Friese Front Formation (SLCF) and Oysterground Member (SLCTO) in well M04-01 in second column; extremely high calculated porosity values in third column (gamma ray log in first column).

The Scruff and Schieland Groups of well L02-05 show an extremely low bulk density log, with values around 2.0 g/cm^3 over large intervals. Calculated porosity values of these litho-stratigraphic groups as a consequence results in extremely high values approaching 0.40. As such values hardly occur in unconsolidated sandstone, the calculated results for this well seem not realistic.

Care should be taken in applying calculation methods to either other stratigraphical intervals or lateral occurrences of the same formation. Expanding the established relationship to other formations is ambiguous as matrix properties may differ substantially from the formations and lithologies used for calibration. As sand-shale parameters are used in the applied calculations, the presence of other matrix material (e.g. evaporites or coal) would result in erroneous porosities. This is exemplified with the presence of impermeable Zechstein salts, that may show relatively low bulk densities down to 2.0 g/cm^3 resulting in calculation of overestimated porosities over 40% using sand-shale density parameters. Hence, above methods are only to be applied to sand-shale intervals.

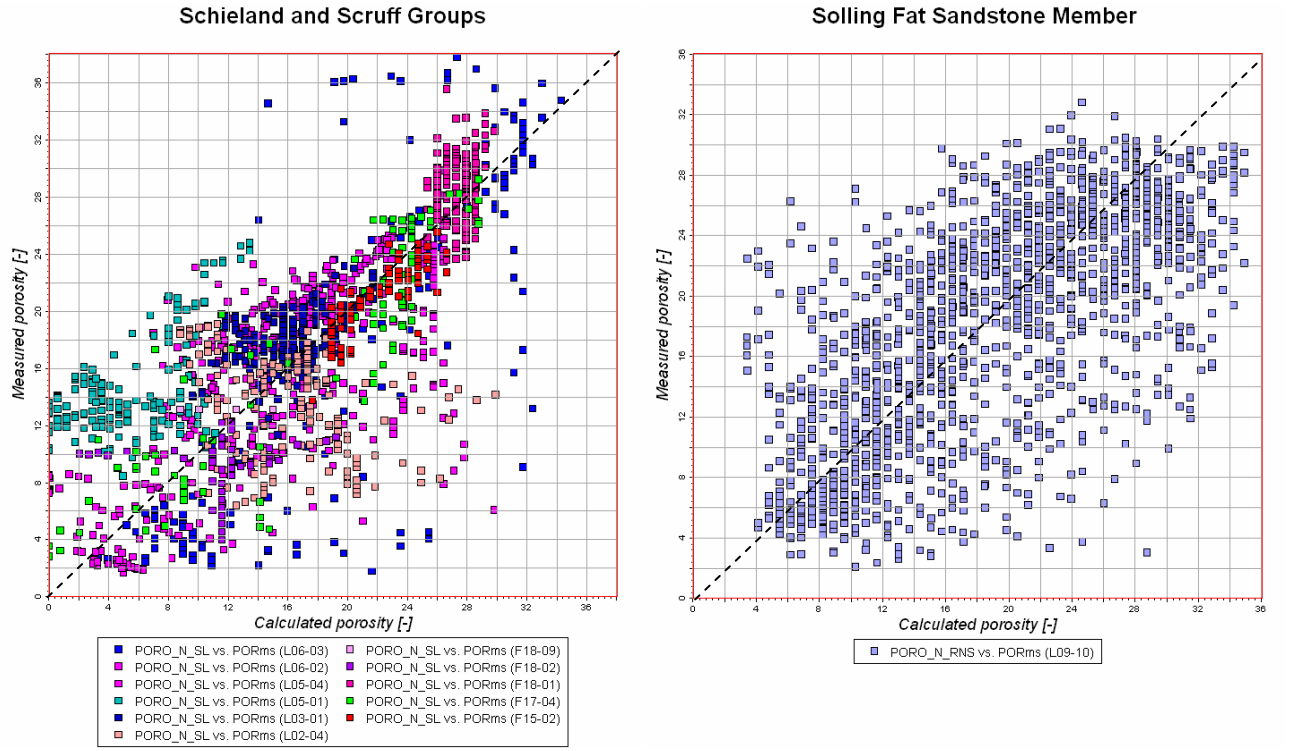

a. Schieland and Scruff Groups (SL) for eleven wells

b. Solling Fat Sandstone member (RNSOF) for single well

c. Main Buntsandstein Subgroup (RBM) for five wells

d. Upper Rotliegend Group (RO) for eight wells

Figure 10. Cross plots of calculated porosity versus available measured values for different potential reservoir levels of the Terschelling Basin and southern Central North Sea Graben region. The dotted lines represent ideal correlation between measurements and calculation results.

Even the application of calibrated relationships to the same formation at other locations needs to be handled with care as lateral variations and local effects may cause deviations from material parameters used in the determination. Local cementation or lateral grain size fluctuation result in different conditions and misleading porosity values. However, in general measured densities do not vary substantially within litho-stratigraphic units as shown in the distribution curves of figure 4.

The calculated porosity results in general show good correlation to values measured from core-plugs (figure 10). A roughly linear relation can be distinguished for all investigated levels. For the Schieland and Scruff Groups (figure 10a) most of the evaluated wells comply with the measurements, although the data of L02-04 and L05-01 are slightly deviated.
The Solling Fat Sandstone member (figure 10b) shows a very broad distribution, but still inhibits a clear trend along the correlation line displayed in the cross plot. The scattering can be explained by the fact that measurements on this interval for well L09-10 show higher detail and more extreme values relative to the calculation that seems to have somewhat smoothed the results. This effect is discussed above and can be observed in the third column of figure 5 that displays this specific well and litho-stratigraphic unit. Nevertheless, the mean value of both measured and calculated porosity is comparable.
Correlation between measurements and calculated results for the Main Buntsandstein Subgroup again show fairly good results (figure 10c). However, data from well L02-02 suggest that calculation slightly underestimated the true, measured porosity.
Porosity calculations on the Upper Rotliegend litho-stratigraphic units correlate nicely to measured values on these intervals as well (figure 10d). Only calculated results of wells L12-02 and M08-01 record a somewhat overestimated porosity.

In general terms the porosity values that were to a large extent calculated in generic manner with the method described in this paper are in good agreement with measured data wherever available. Based on these results, also the quality of porosity calculations on intervals that have not been sampled can be treated with sufficient confidence.

10 Permeability determination

Determination of permeability has not been a final objective of this study, as the uncertainty related to permeability calculation from porosity are fairly high. Especially if the porosity values themselves are derived from other parameters, the error propagation would be too high. Moreover, little measured data is available to calibrate calculated values. Based on these considerations, it is believed that performing such an exercise at this stage would not be opportune.

11 Conclusions

As part of TNO's thematic mapping programme of the Dutch offshore, this study focuses on calculation of petrophysical parameters, porosity in particular, of several potential reservoir levels of the NCP-2A region, such as of the Jurassic Schieland and Scruff Groups, the Upper Germanic Triassic Solling Fat Sandstone member, the Lower Detfurth and Volpriehausen Sandstone Members of the Lower Germanic Triassic Group and the Upper Rotliegend Slochteren Formation. Bulk density logs are favoured over sonic and neutron logs to calculate porosity values for the reasons stated below:

- the existence of a clear and linear theoretical relationship between bulk density and porosity;
- the availability of high resolution data on matrix densities for cored intervals in many litho-stratigraphic units of multiple wells;
- the possibility to evaluate fluid density values directly from resistivity measurements.

The bulk density log is an adequate tool to calculate porosity. However, if the bulk density correction log value (DRHO) exceeds 0.15 or -0.15 g/cm^3 or if the bulk density log itself shows values below 2.0 g/cm^3, the bulk density log is automatically disregarded as its accuracy can no longer be trusted. For certain litho-stratigraphic units of the Schieland Group values below 2.2 g/cm^3 are ignored since the presence of organic rich or coal layers in these units with bulk densities between 2.0-2.2 g/cm^3 can result in overestimation of porosity.

The matrix density for specific litho-stratigraphic units and the pore fluid density for individual wells are derived from core-plug measurements and resistivity analysis, respectively. The influence of the presence of gas in specific litho-stratigraphic units is corrected for by applying the average value of both neutron and bulk density log derived porosity values. In addition, the influence of shale on the average porosity is minimized using the net reservoir intervals only, distinctive from the remaining part of the units by its lower shale content, expressed in lower gamma ray log values.

Especially for deeper, heavily compressed reservoirs the calculation results seem to be in very good agreement with expected values. For the more shallow units of the Scruff and Schieland Groups results are also corresponding to measurements, but errors may be somewhat larger due to lesser compression. This approach, therefore, effectively quantifies porosity values primarily using the bulk density log.

The calculated porosity values show, where possible, close correlation to measured values, although in a few single cases the match is somewhat less close slightly overestimating or underestimating the true porosity. However, in general the calculated results are in very good agreement with measured values. Therefore, this study can be regarded as a valuable conversion of well log data to petrophysical properties for the Terschelling Basin and southern Central North Sea Graben region potential reservoir intervals. In the future a similar approach can be applied on other regions or stratigraphic levels, provided that sufficient input data is available.

References

Abbink, O.A., Mijnlieff, H.F., Munsterman, D.K. and Verreussel, R.M.C.H., 2006. New stratigraphic insights in the 'Late Jurassic' of the Southern Central North Sea Graben and Terschelling Basin (Dutch Offshore) and related exploration potential. Netherlands Journal of Geosciences – Geologie en Mijnbouw, 85(3), 221-238.

Ramaekers, J.J.F., 2006. Personal communication.

Rider, M.H., 1986. The geological interpretation of well logs. John Wiley & Sons, New York, 175 p. Revised edition, 2002: Rider-French Consulting Ltd., Scotland, 280 p.

Stegers, D.P.M., 2006. Sedimentary facies analysis of sequence 2 of the Upper Jurassic in the Terschelling Basin and the southern Dutch Central Graben. TNO Report 2006-U-R0191/A, TNO, 43 p.

Verreussel, R.M.C.H. and Munsterman, D.K., 2006. Personal communication.

Signature

Utrecht, the Netherlands
February 14, 2007

TNO Built Environment and Geosciences
Geological Survey of the Netherlands

J.C. Doornenbal
Group leader

T. Benedictus
Author

Appendix I - Porosity logs

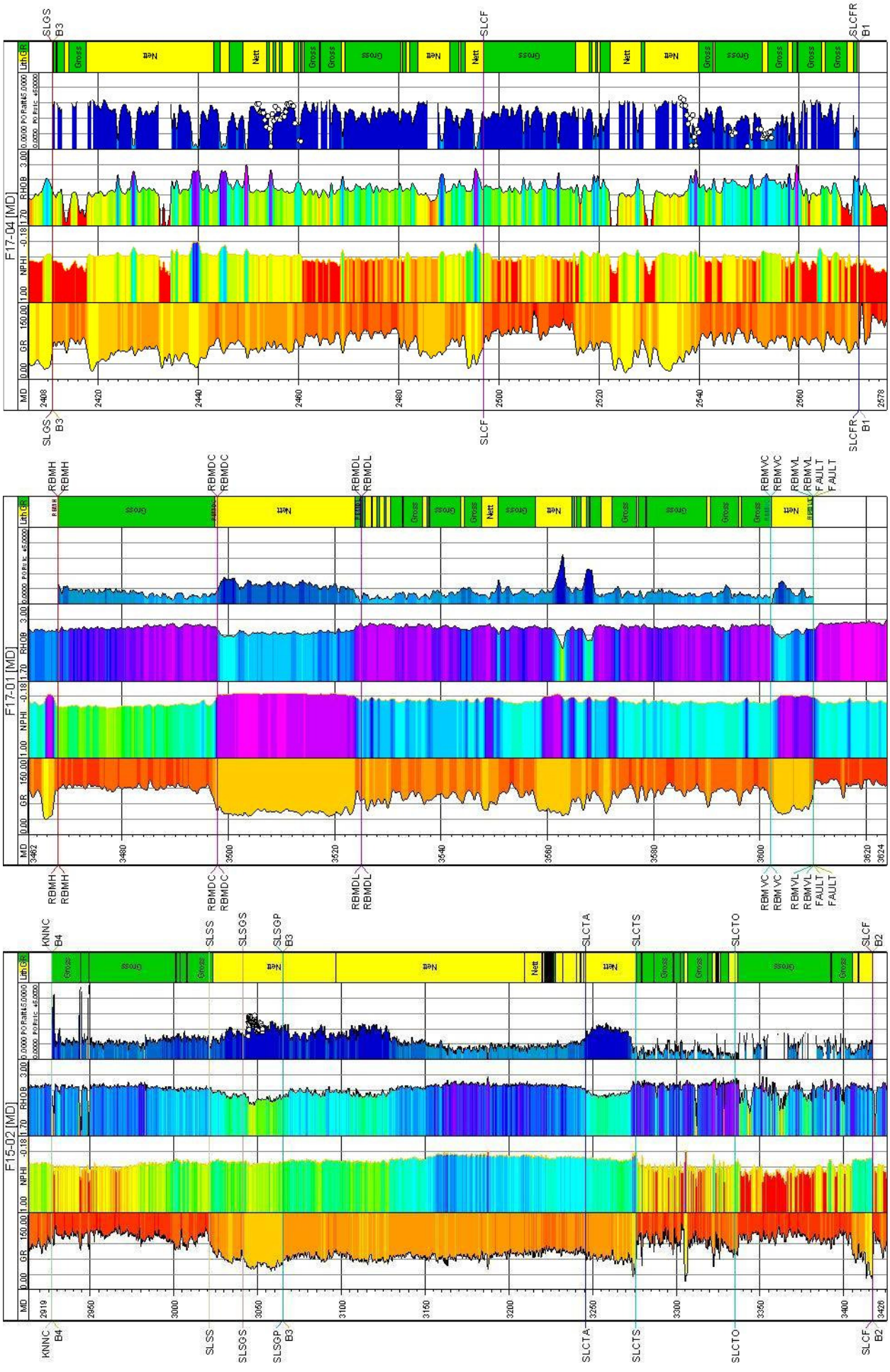
F17-04 [MD]
SLGS B3
SLCF
SLCFR B1
F17-01 [MD]
RBMH
RBMDC
RBMDL
RBMVC
RBMVL
FAULT
F15-02 [MD]
KNNC B4
SLSS
SLSGS
SLSGP B3
SLCTA
SLCTS
SLCTO
SLCF B2

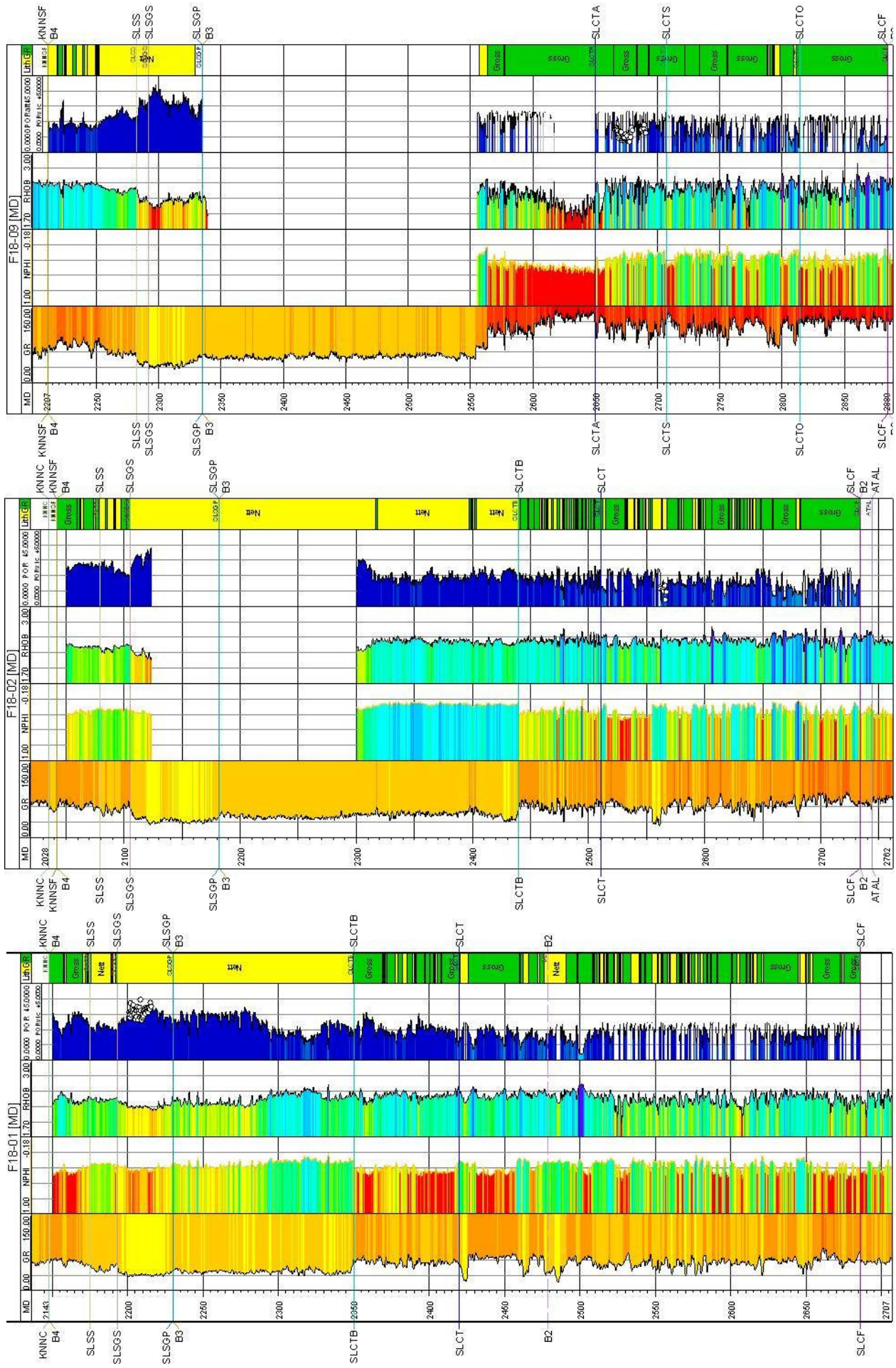
F18-09 [MD]
F18-02 [MD]
F18-01 [MD]
KNNSF
B4
SLSS
SLSGS
SLSGP
B3
SLCTA
SLCTS
SLCTO
SLCF
KNNC
SLCTB
SLCT
B2
ATAL
Gross
Net
LithGR
POR
RHOB
NPHI
GR
MD

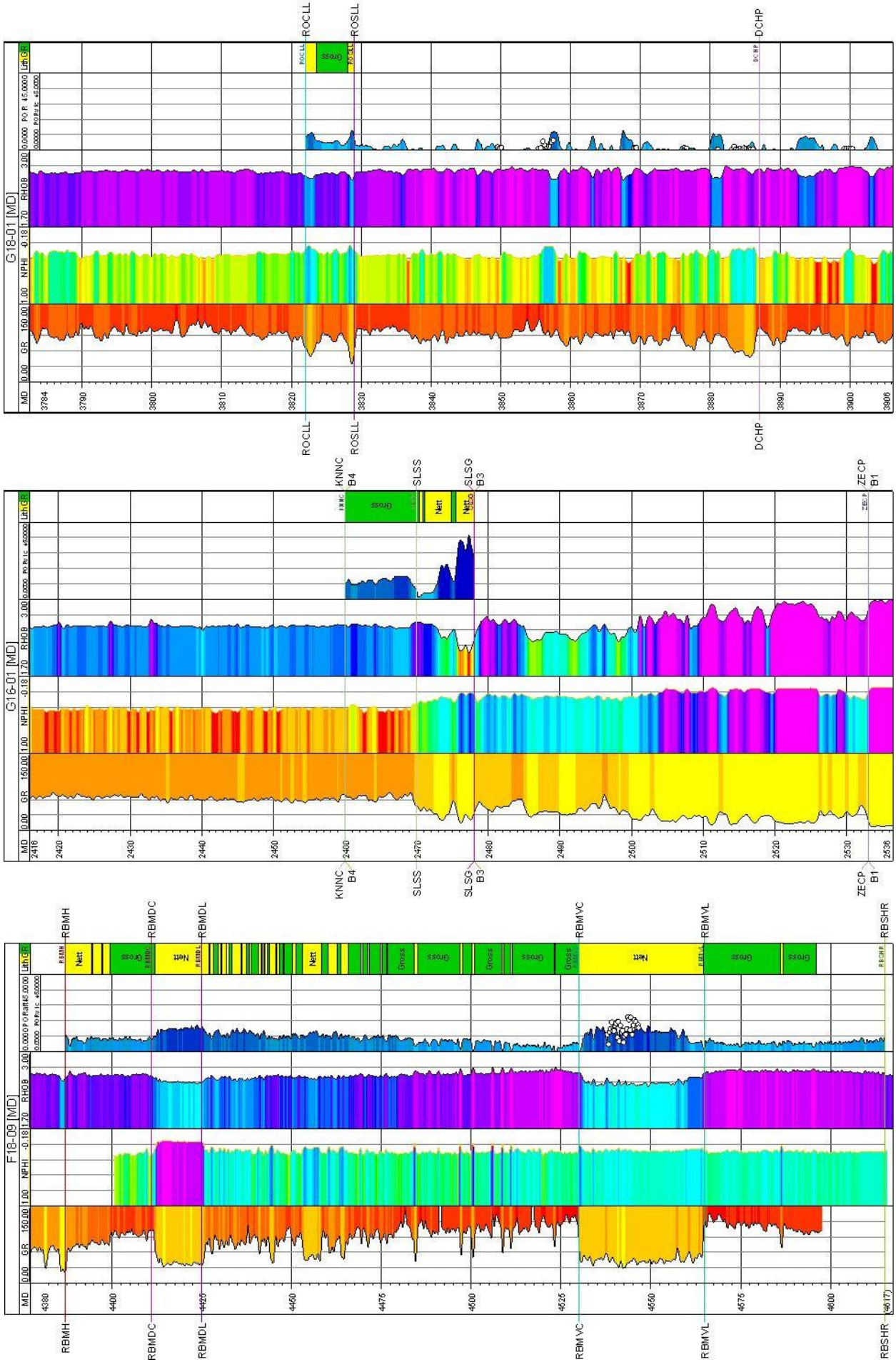
ROCLL
ROSLL
DCHP
G18-01 [MD]
KNNC
B4
SLSS
SLSG
B3
ZECP
B1
G16-01 [MD]
RBMH
RBMDC
RBMDL
RBMVC
RBMVL
RBSHR
F18-09 [MD]

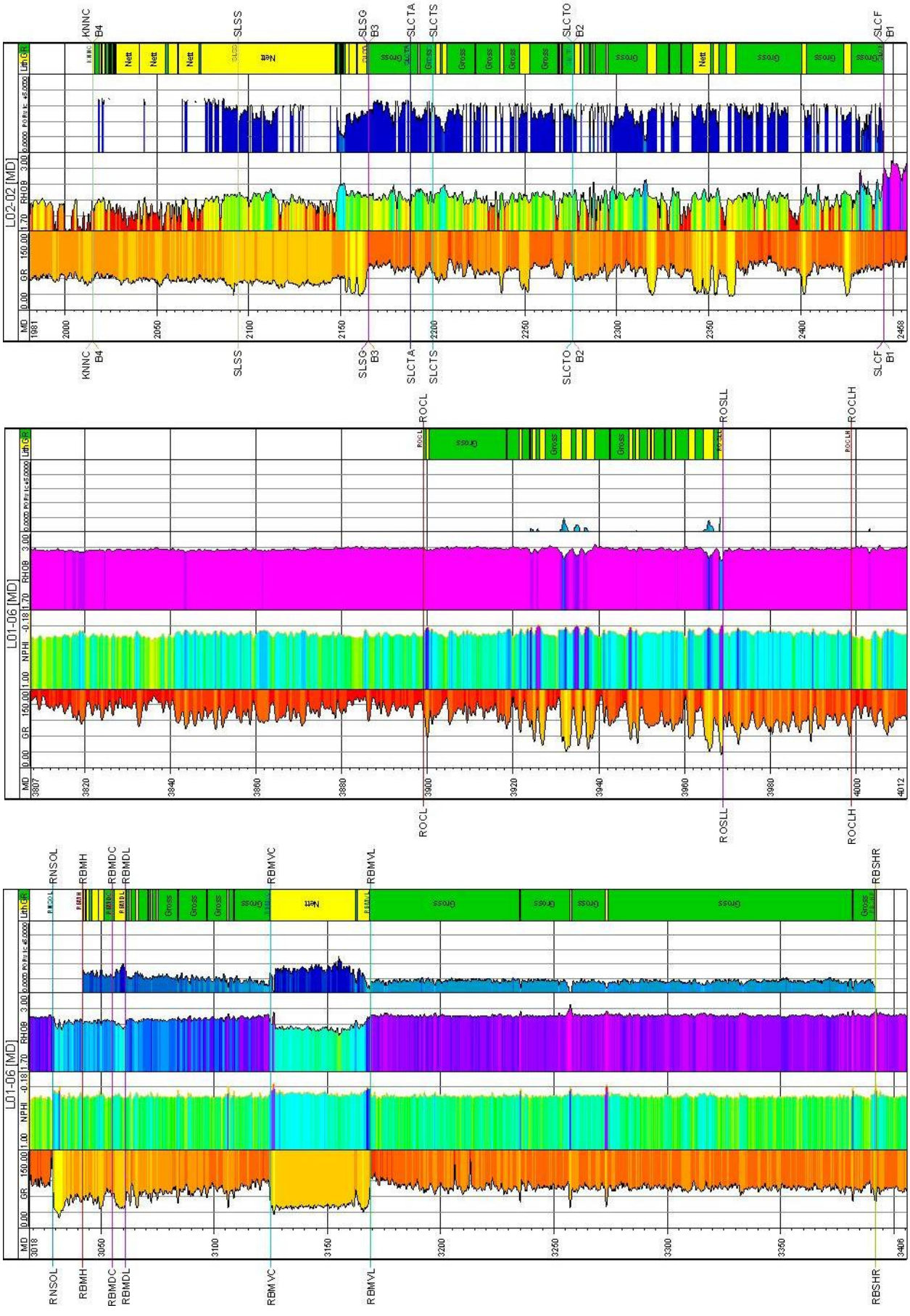
KNNC
B4
SLSS
SLSG
B3
SLCTA
SLCTS
SLCTO
B2
SLCF
B1
L02-02 [MD]
LithGR
RHOB
GR
MD
Net
Gross
ROCL
ROSLL
ROCLH
L01-06 [MD]
NPHI
RNSOL
RBMH
RBMDC
RBMDL
RBMVC
RBMVL
RBSHR

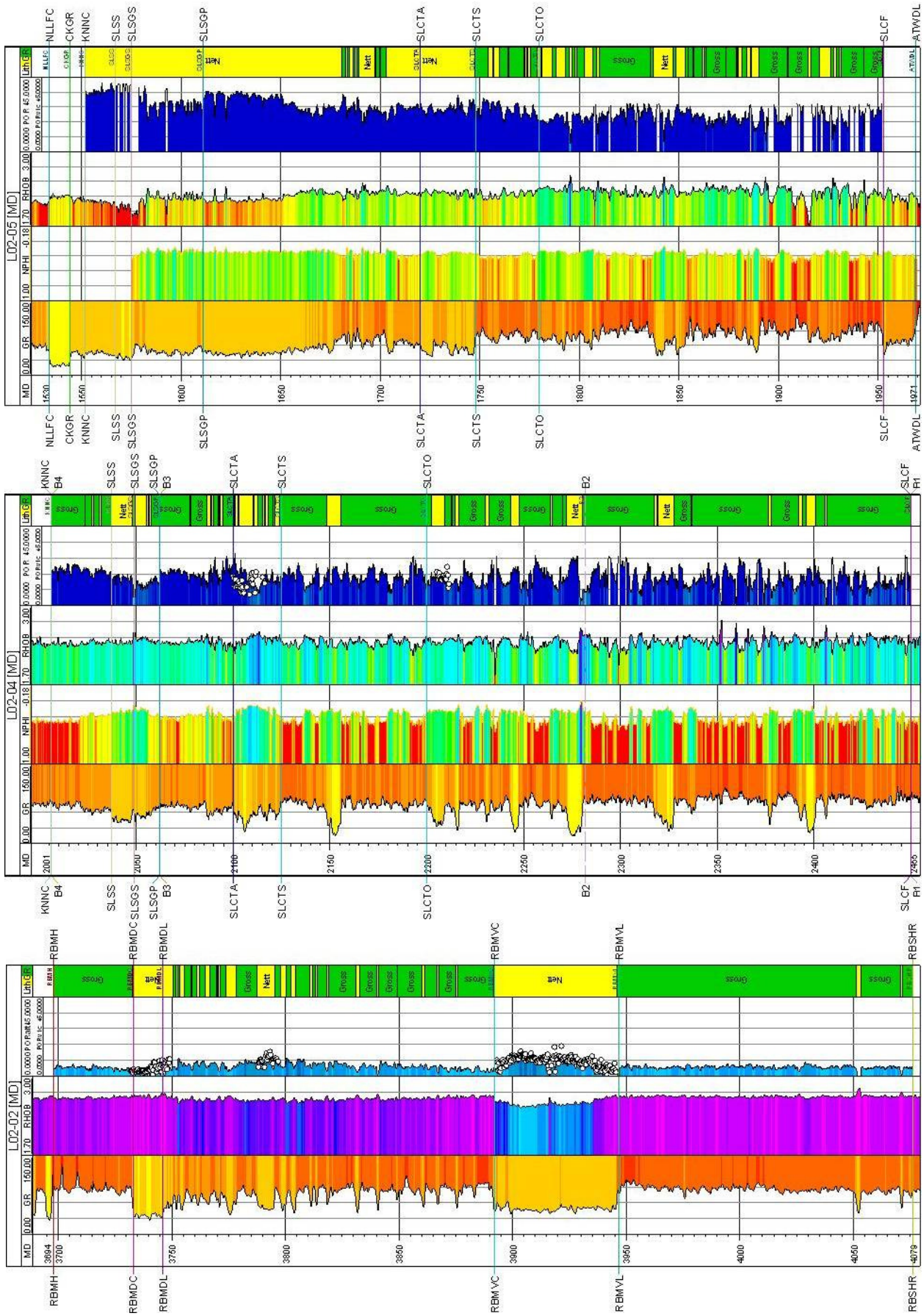
L02-05 [MD]
NLLFC
CKGR
KNNC
SLSS
SLSGS
SLSGP
SLCTA
SLCTS
SLCTO
SLCF
ATWDL
L02-04 [MD]
KNNC
B4
SLSS
SLSGS
SLSGP
B3
SLCTA
SLCTS
SLCTO
B2
SLCF
R1
L02-02 [MD]
RBMH
RBMDC
RBMDL
RBMVC
RBMVL
RBSHR

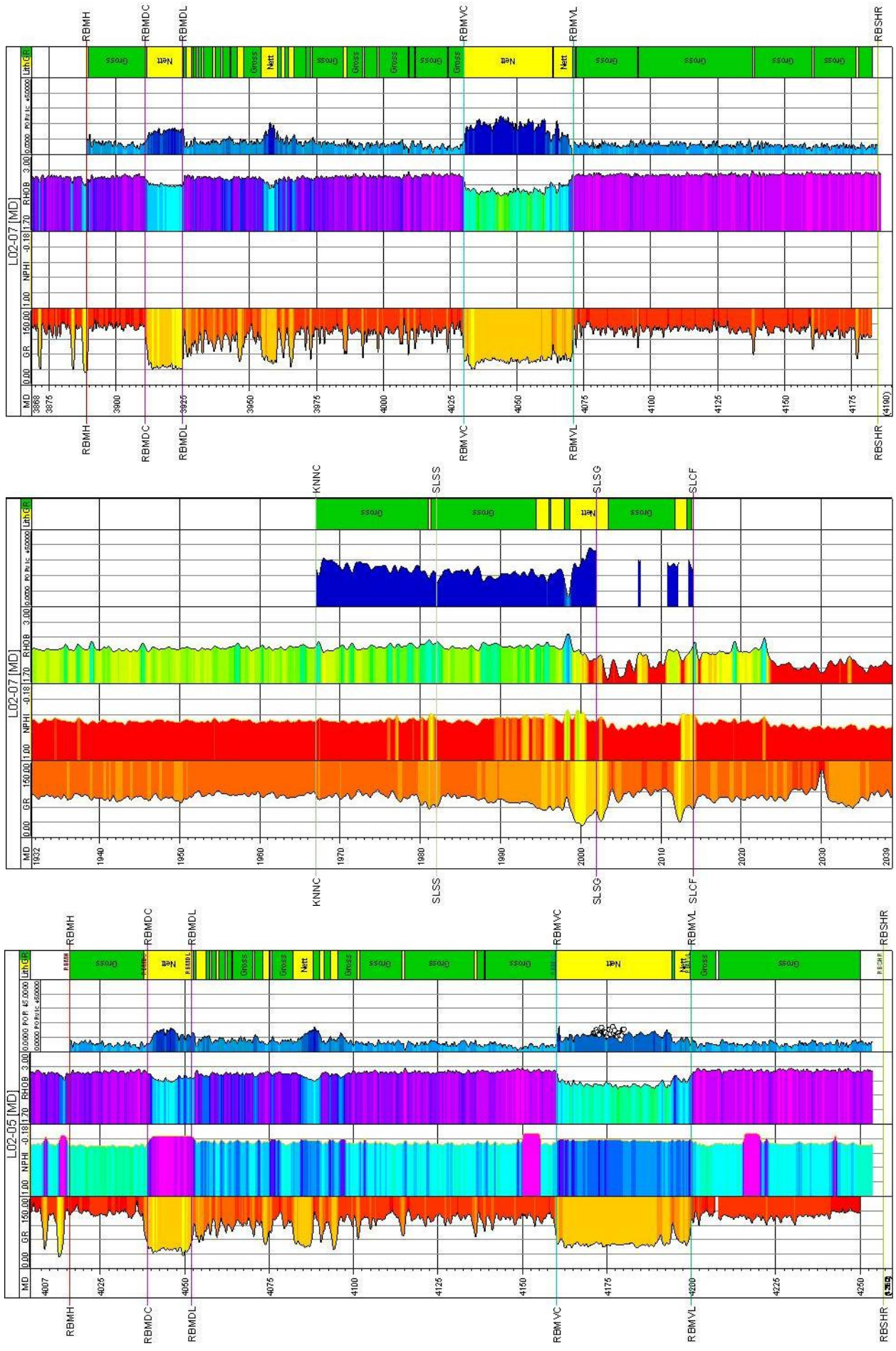
RBMH
RBMDC
RBMDL
RBMVC
RBMVL
RBSHR
L02-07 [MD]
LithGR
RHOB
NPHI
GR
MD
KNNC
SLSS
SLSG
SLCF
L02-05 [MD]

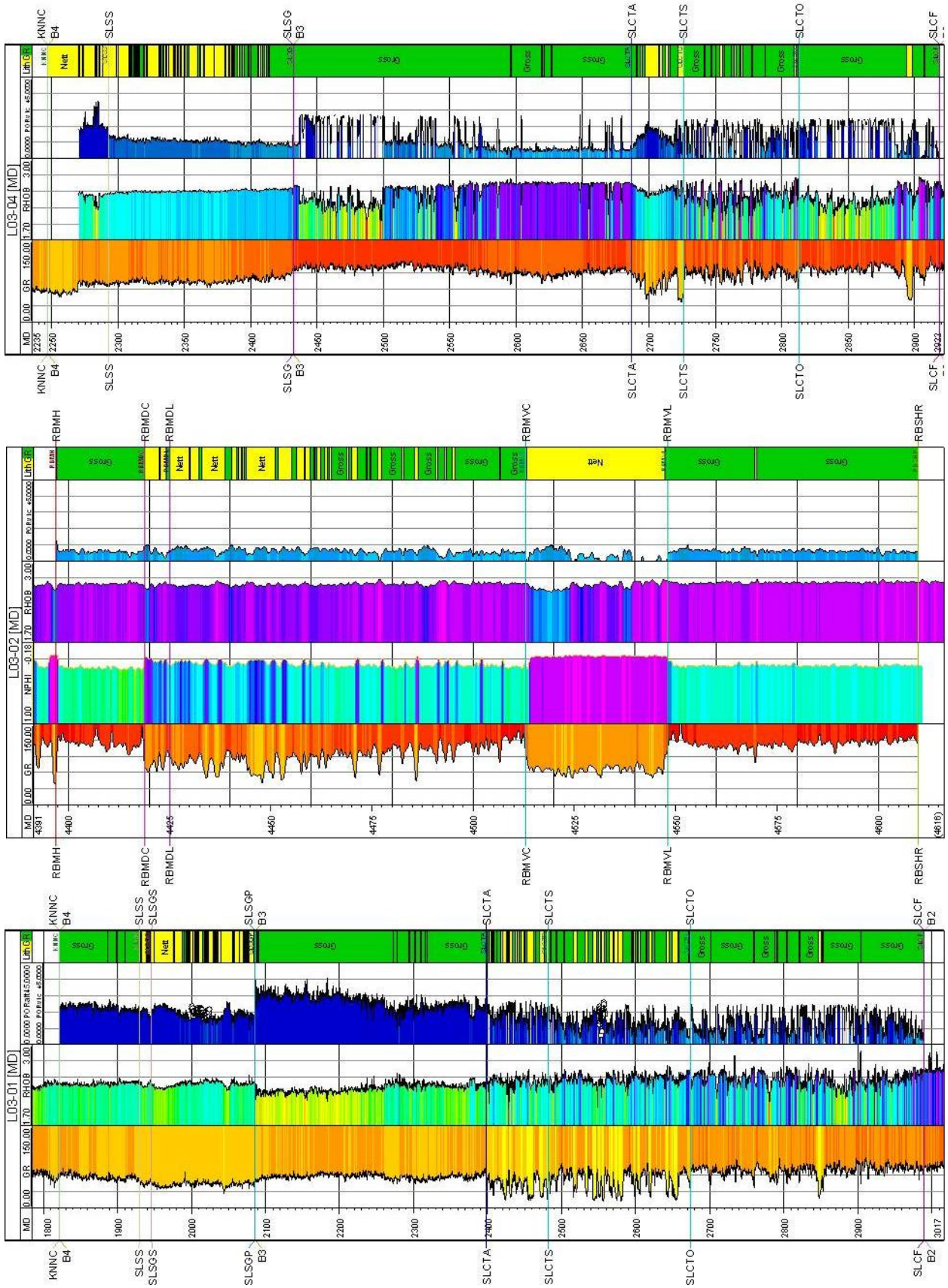
KNNC
B4
SLSS
SLSG
B3
SLCTA
SLCTS
SLCTO
SLCF
L03-04 [MD]
Lith GR
Net
Gross
RHOB
GR
MD
RBMH
RBMDC
RBMDL
RBMVC
RBMVL
RBSHR
L03-02 [MD]
NPHI
SLSS
SLSGS
SLSGP
B2
L03-01 [MD]

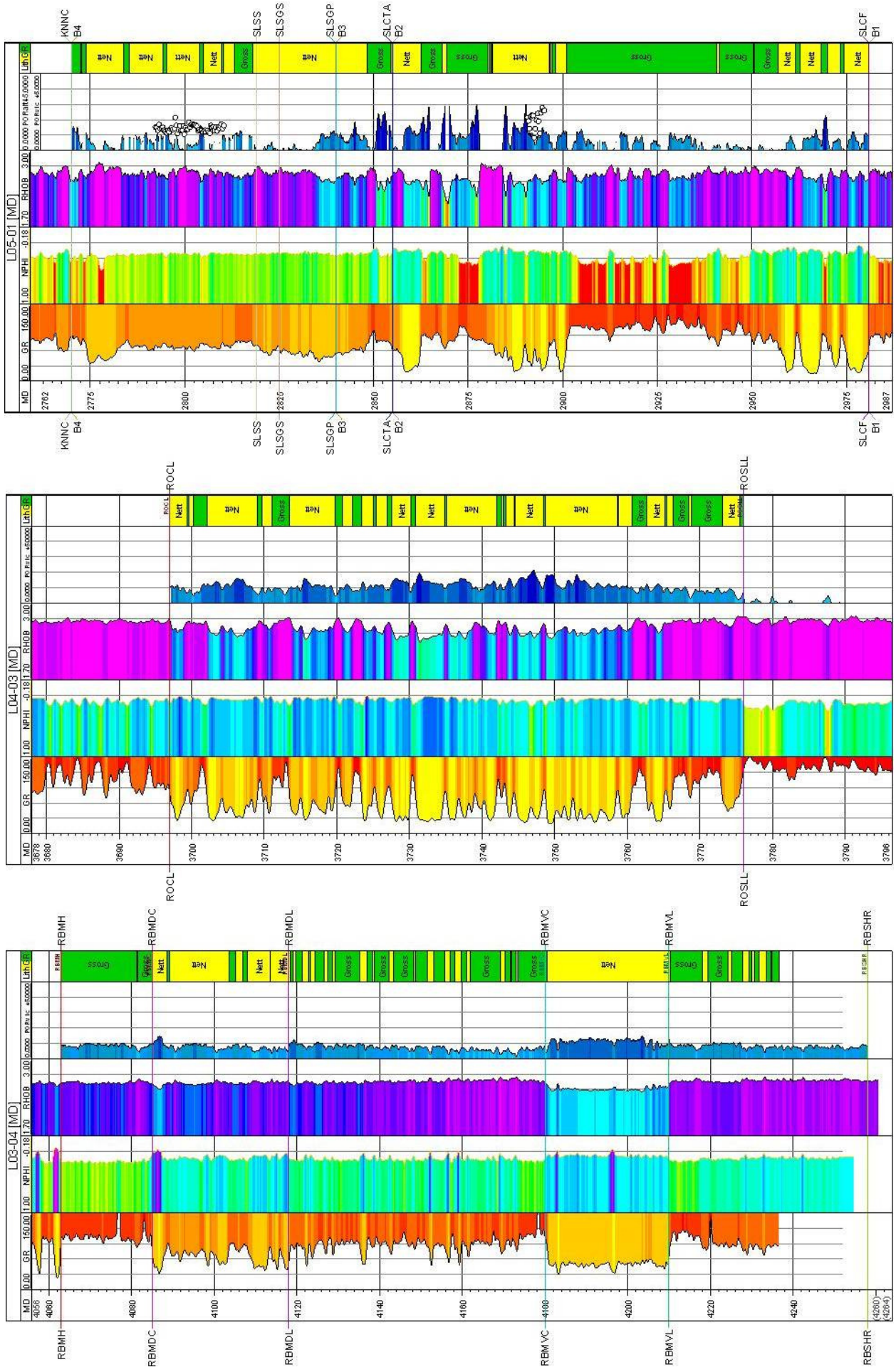
KNNC
B4
SLSS
SLSGS
SLSGP
B3
SLCTA
B2
SLCF
B1
L05-01 [MD]
ROCL
ROSLL
L04-03 [MD]
RBMH
RBMDC
RBMDL
RBMVC
RBMYL
RBSHR
L03-04 [MD]

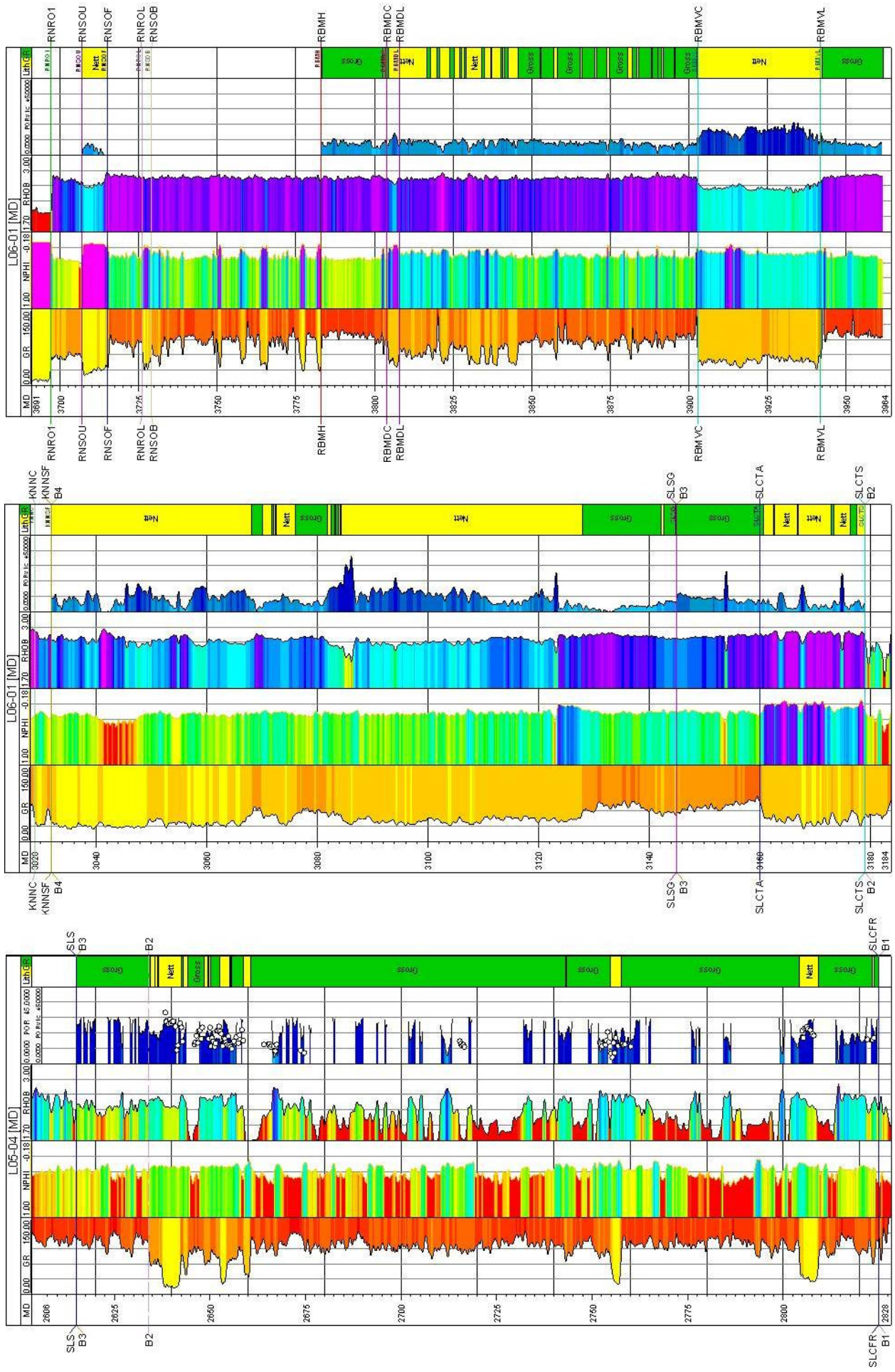
RNRO1
RNSOU
RNSOF
RNROL
RNSOB
RBMH
RBMDC
RBMDL
RBMVC
RBMVL
L06-01 [MD]
KNNC
KNNSF
B4
SLSG
B3
SLCTA
SLCTS
B2
L06-01 [MD]
SLS
B3
B2
SLCFR
B1
L05-04 [MD]

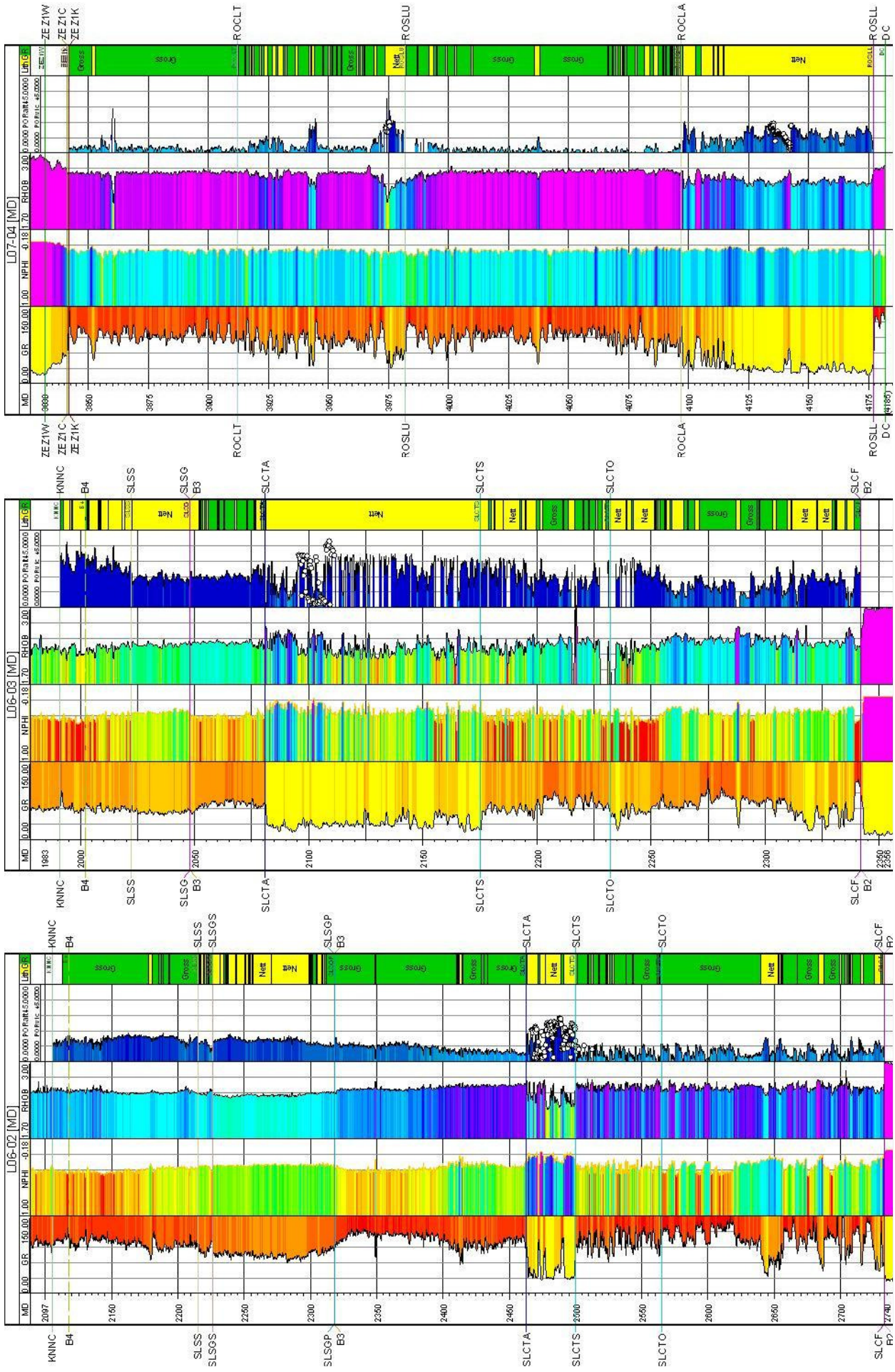
L07-04 [MD]
ZEZ1W
ZEZ1C
ZEZ1K
ROCLT
ROSLU
ROCLA
ROSLL
D C
L06-03 [MD]
KNNC
B4
SLSS
SLSG
B3
SLCTA
SLCTS
SLCTO
SLCF
B2
L06-02 [MD]
KNNC
B4
SLSS
SLSGS
SLSGP
B3
SLCTA
SLCTS
SLCTO
SLCF
B2

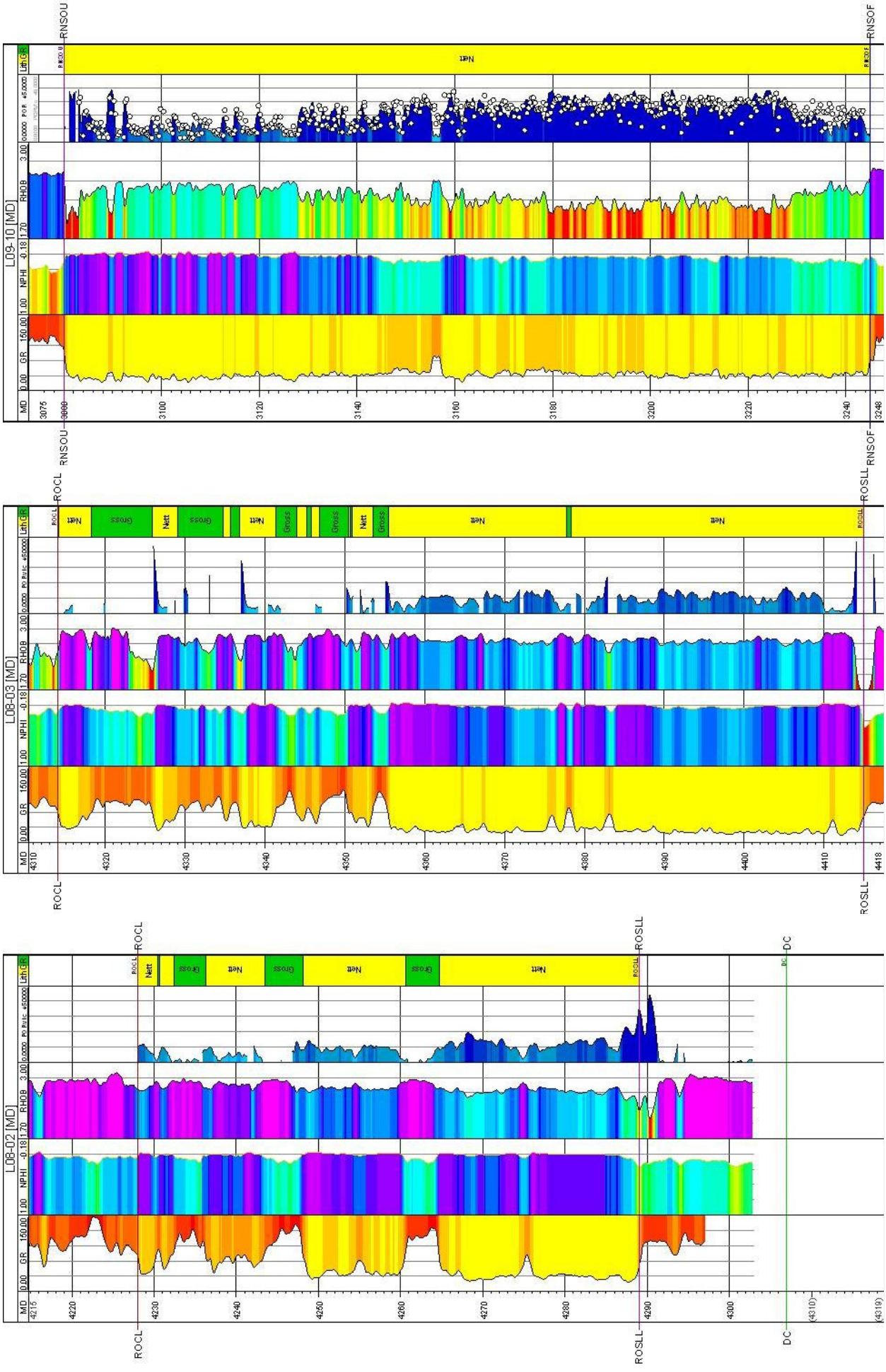
RNSOU
RNSOF
L09-10 [MD]
Net
LithGR
RHOB
NPHI
GR
MD
ROCL
ROSLL
L08-03 [MD]
Net
Gross
Nett
L08-02 [MD]
DC

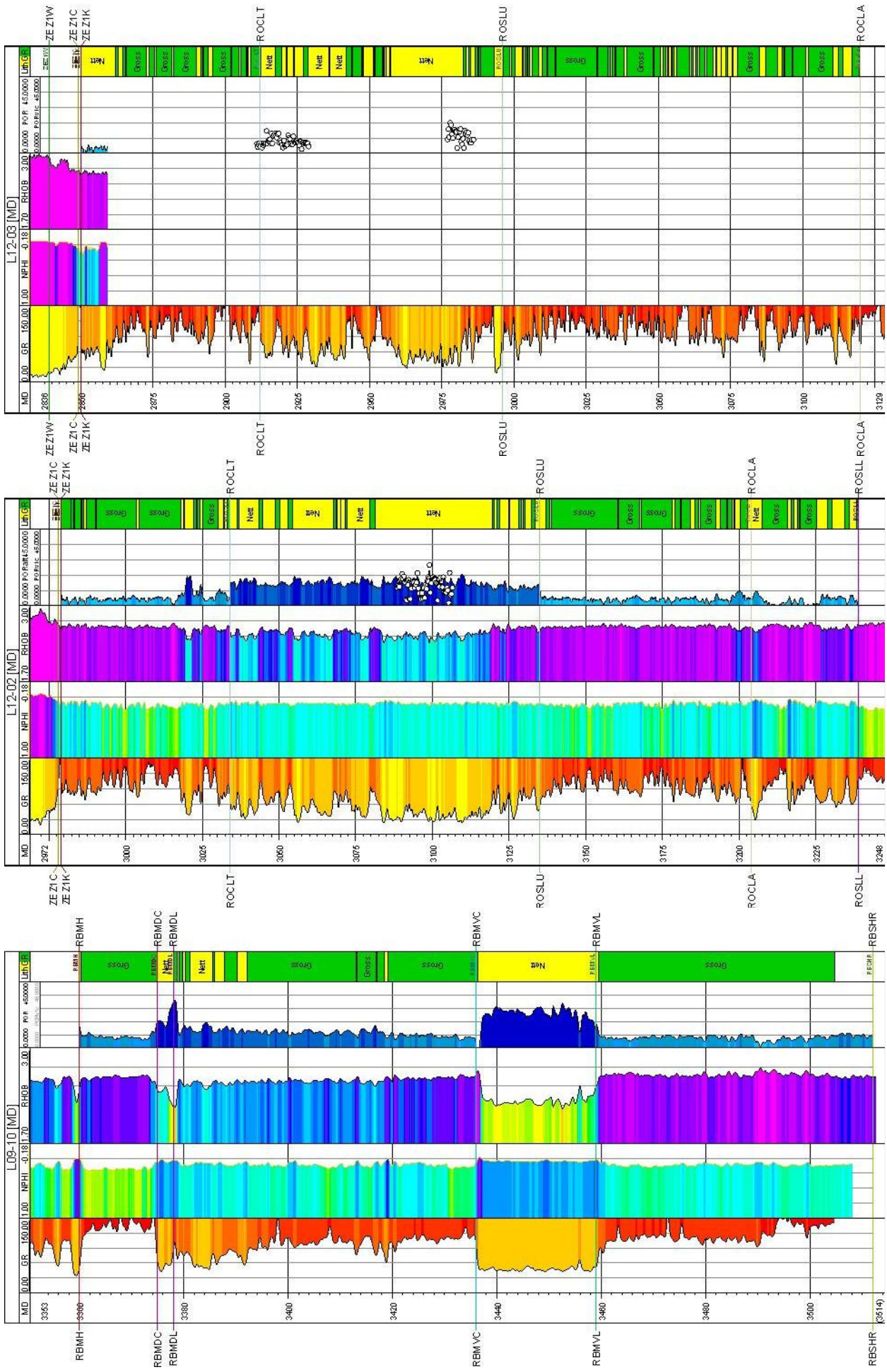
L12-03 [MD]
ZE Z1W
ZE Z1C
ZE Z1K
ROCLT
ROSLU
ROCLA
L12-02 [MD]
ROSLL
L09-10 [MD]
RBMH
RBMDC
RBMDL
RBMVC
RBMVL
RBSHR

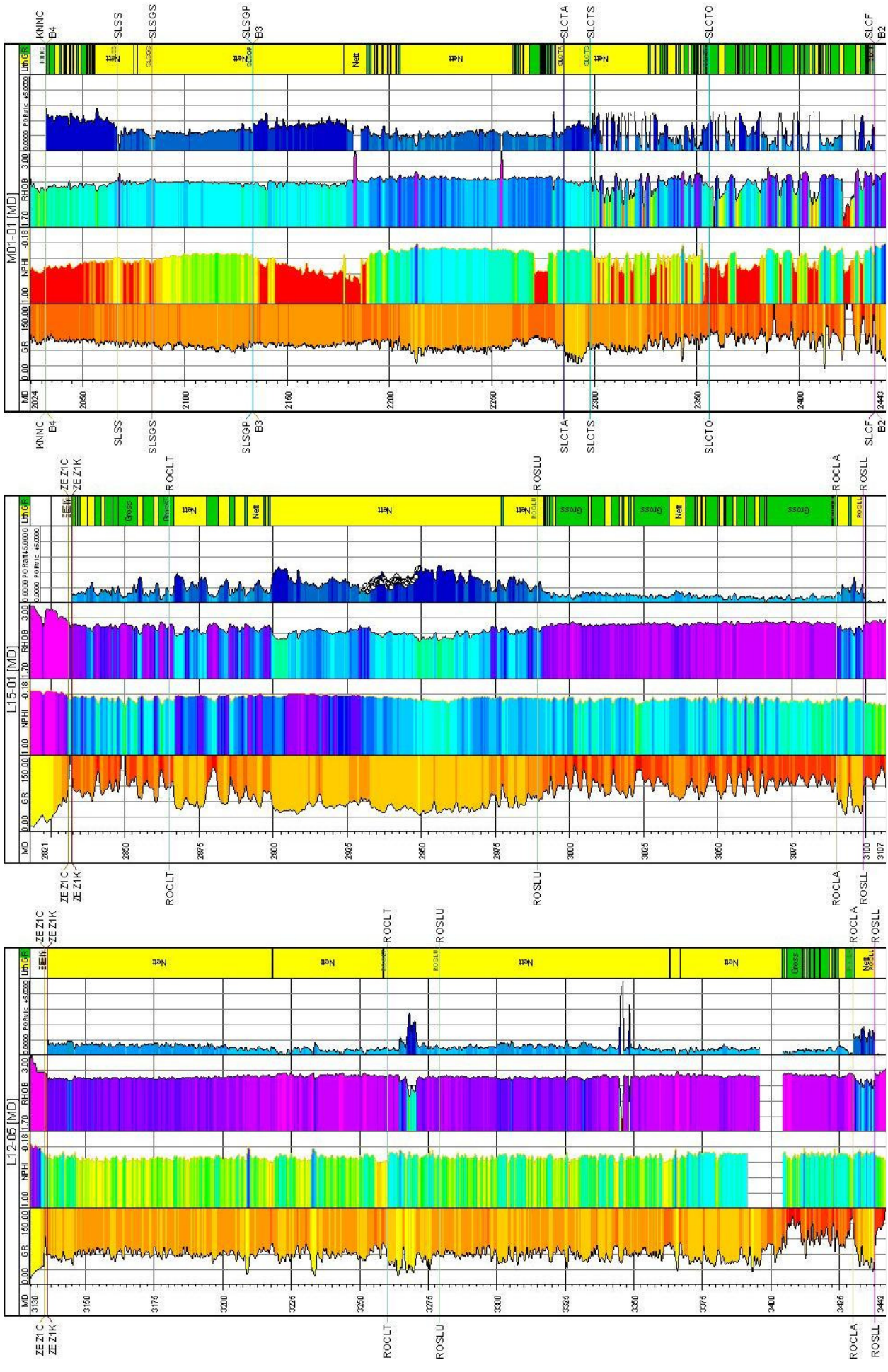
M01-01 [MD]
KNNC
B4
SLSS
SLSGS
SLSGP
B3
SLCTA
SLCTS
SLCTO
SLCF
B2
L15-01 [MD]
ZE Z1C
ZE Z1K
ROCLT
ROSLU
ROCLA
ROSLL
L12-05 [MD]

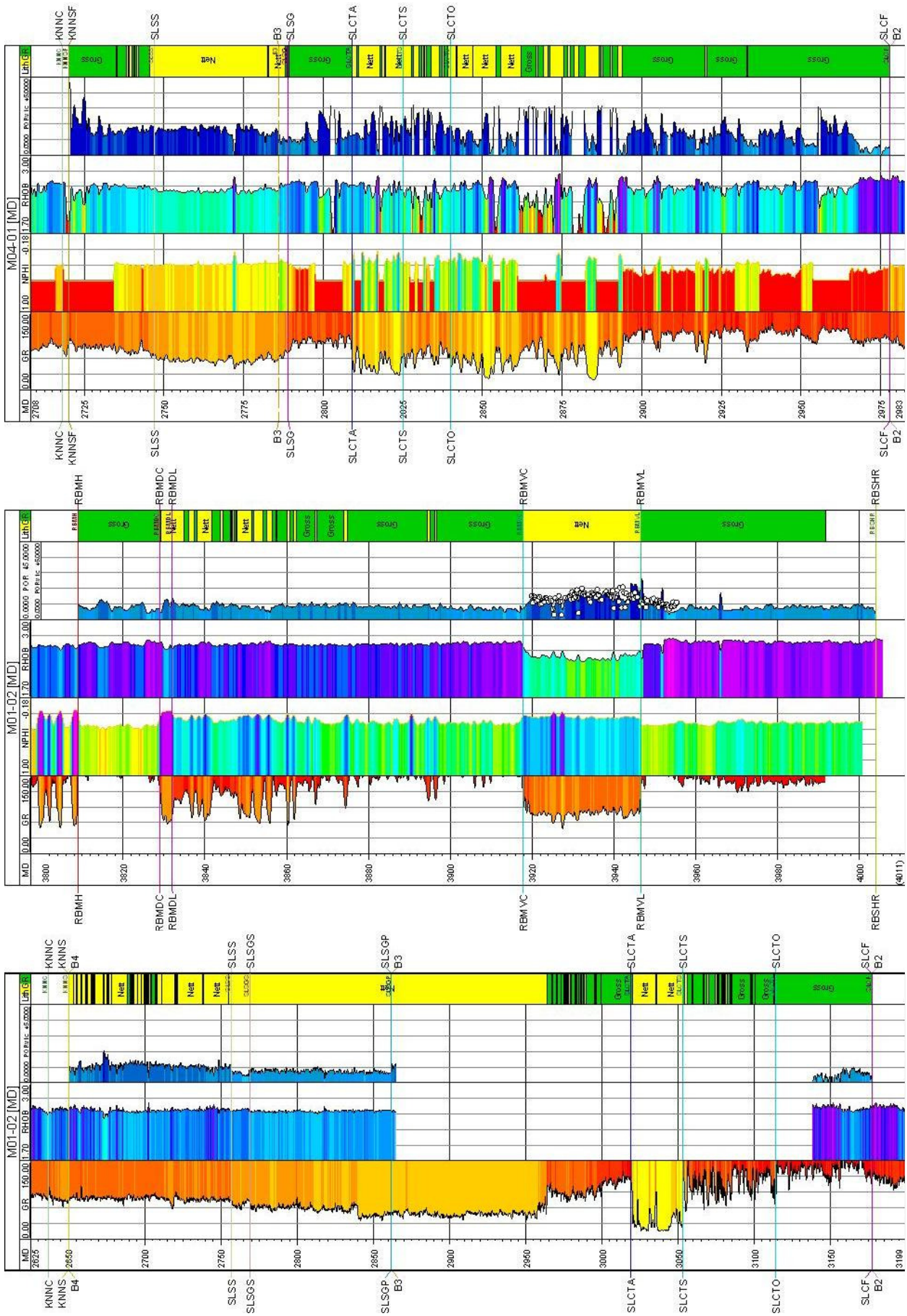
KNNC
KNNSF
SLSS
B3
SLSG
SLCTA
SLCTS
SLCTO
SLCF
B2
M04-01 [MD]
Lith.GR
Gross
Nett
RHOB
NPHI
GR
MD
RBMH
RBMDC
RBMDL
RBMVC
RBMYL
RBSHR
M01-02 [MD]
KNNS
B4
SLSGS
SLSGP

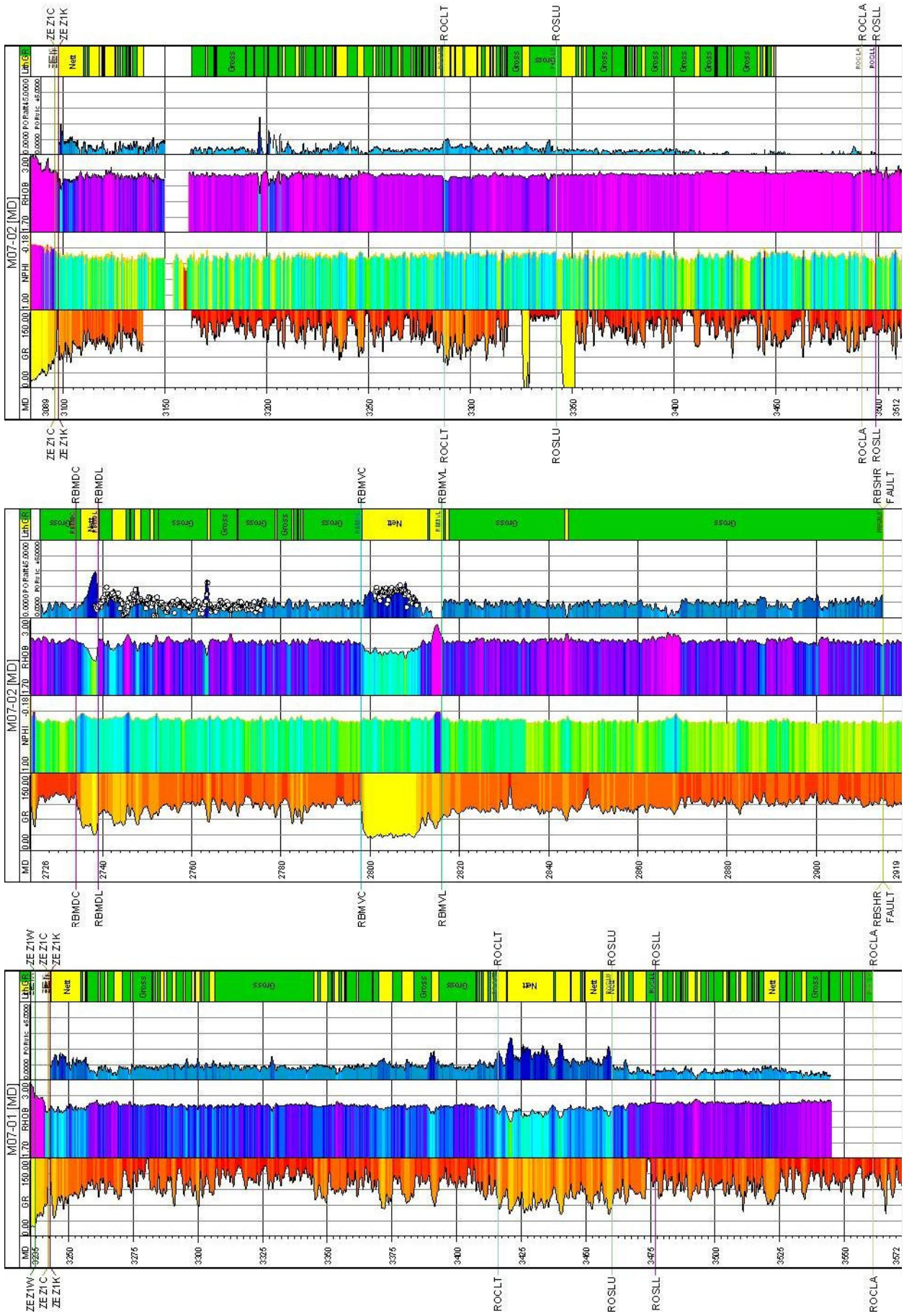
MD
GR
NPHI
RHOB
PORT
Gross
Net
ZE Z1C
ZE Z1K
ROCLT
ROSLU
ROCLA
ROSLL
RBMDC
RBMDL
RBMVC
RBMVL
RBSHR
FAULT
MD07-02 [MD]
MD07-01 [MD]
ZE Z1W

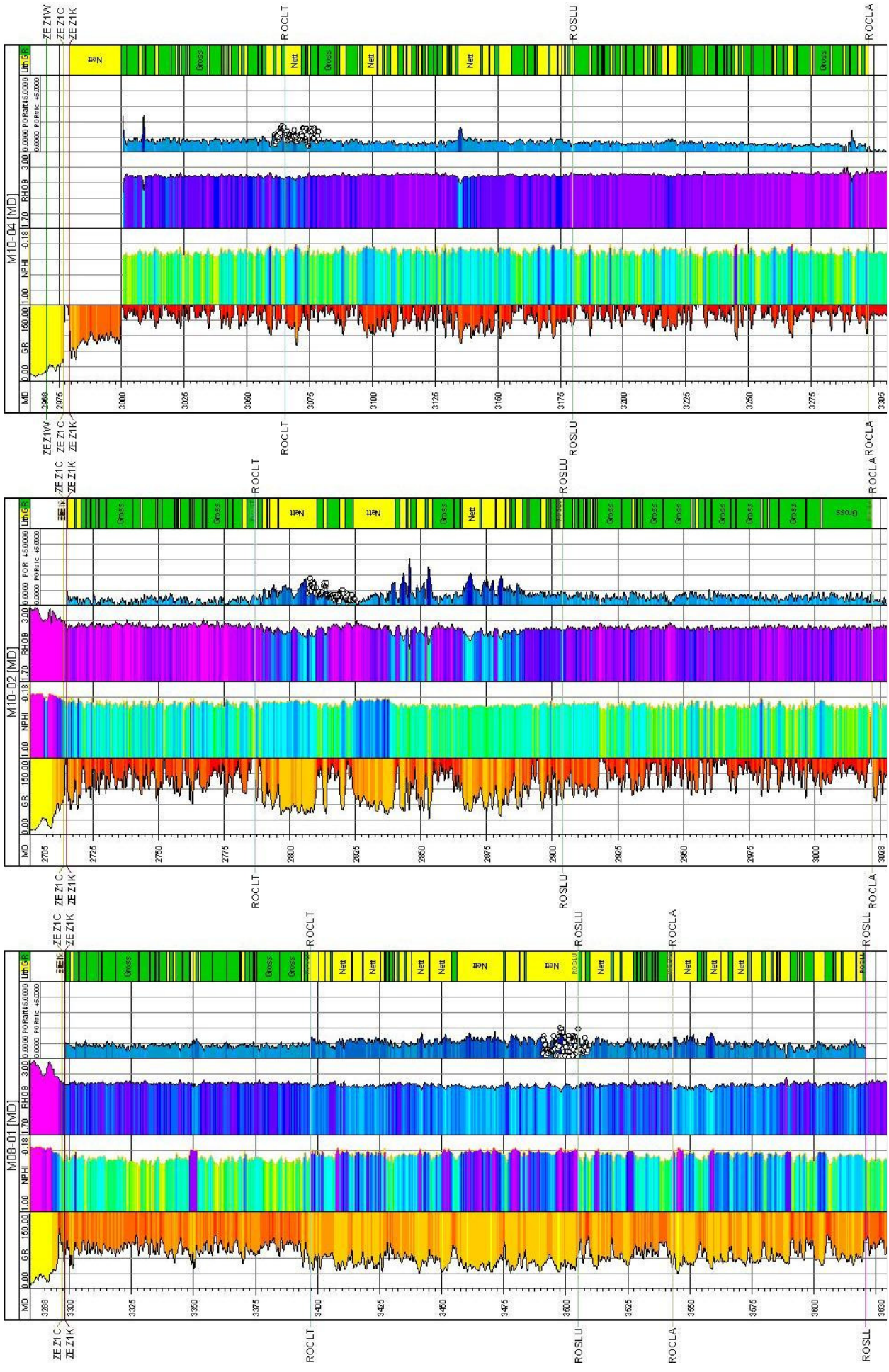
M10-04 [MD]
M10-02 [MD]
M08-01 [MD]
ZE Z1W
ZE Z1C
ZE Z1K
ROCLT
ROSLU
ROCLA
ROSLL
Net
Gross
Nett
GR
NPHI
RHOB
MD

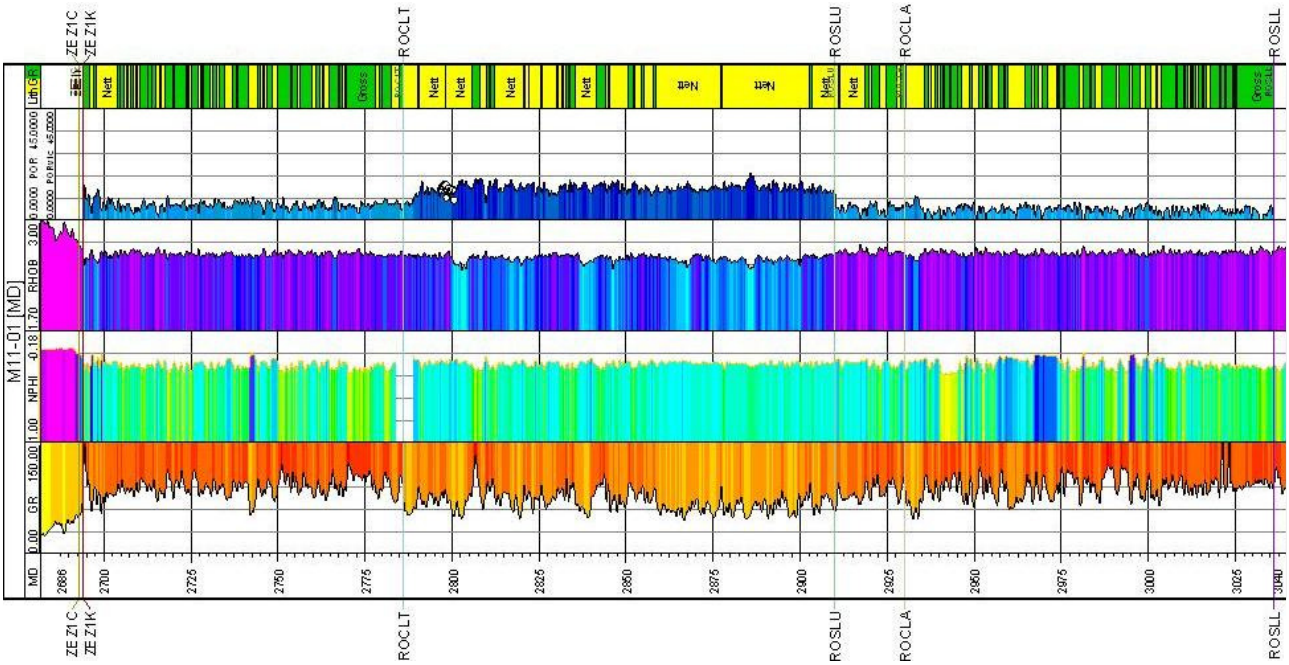
ZE Z1C
ZE Z1K
ROCLT
ROSLU
ROCLA
ROSLL
M11-01 [MD]
Litho
Net
Gross
POR
PORIrc
RHOB
NPHI
GR
MD
2675
2700
2725
2750
2775
2800
2825
2850
2875
2900
2925
2950
2975
3000
3025
3040

Appendix II - Mean net porosity

Mean porosity and standard deviation of potential reservoir units for wells in or adjacent to the Terschelling Basin and southern Central North Sea Graben (NCP-2A) region of the Dutch offshore. Values are derived using the arithmetic mean porosity of calculated porosity over net intervals of the investigated reservoirs.

Litho-stratigraphic units		SLSS	SLSG	SLSGS	SLSGP	SLCT	SLCTA	SLCTB	SLCTS	SLCTO	SLCF	SLCFR	RNSOF	RBMDC	RBMDL	RBMVC	RBMVL	RBSHR	ROCLT	ROSLU	ROCLA	ROSLL
F15-02	porosity [%]	12.54 ± 1.20		14.29 ± 2.49	19.72 ± 2.89		10.98 ± 4.43		16.33 ± 3.54	2.61 ± 1.99	6.46 ± 2.94											
	top [m]	2927.0		3021.0	3041.0		3065.0		3246.0	3276.0	3335.0											
	base [m]	3021.0		3041.0	3065.0		3246.0		3276.0	3335.0	3417.0											
	N/G [-]	0.017		0.895	1.000		0.973		1.000	0.188	0.165											
F17-01	porosity [%]													6.59 ± 0.89	11.35 ± 1.91	7.85 ± 5.00	7.71 ± 3.06					
	top [m]		1660.0								1770.0	1815.0		3468.0	3498.0	3525.0	3602.0					
	base [m]		1770.0								1815.0	1870.0		3498.0	3525.0	3602.0	3610.0					
	N/G [-]		0.697								0.902	0.898		0.020	0.963	0.277	0.963					
F17-04	porosity [%]										18.67 ± 7.89	18.80 ± 8.18										
	top [m]										2411.0	2497.0										
	base [m]										2497.0	2572.0										
	N/G [-]										0.583	0.343										
F18-01	porosity [%]	21.57 ± 2.12		19.27 ± 1.53	26.11 ± 2.83	14.83 ± 2.16		21.04 ± 5.42			15.58 ± 3.30											
	top [m]	2148.0		2175.0	2193.0	2350.0		2230.0			2420.0											
	base [m]	2175.0		2193.0	2230.0	2420.0		2350.0			2686.0											
	N/G [-]	0.156		0.872	0.997	0.147		0.996			0.308											
F18-02	porosity [%]	24.14 ± 0.77		22.74 ± 2.30	27.95 ± 3.70	13.87 ± 3.45		18.05 ± 3.25			14.37 ± 4.08											
	top [m]	2042.0		2079.0	2105.0	2440.0		2182.0			2511.0											
	base [m]	2079.0		2105.0	2182.0	2511.0		2440.0			2734.0											
	N/G [-]	0.141		0.615	0.997	0.321		0.983			0.248											
F18-09	porosity [%]	18.34 ± 3.53		26.83 ± 4.00	30.08 ± 3.93		14.87 ± 3.58		14.91 ± 4.24	15.00 ± 5.13				6.95 ± 1.26	12.97 ± 1.25	8.79 ± 3.11	10.40 ± 3.07	4.13 ± 0.65				
	top [m]	2211.0		2282.0	2292.0		2335.0		2650.0	2707.0	2814.0			4387.0	4411.0	4425.0	4530.0	4565.0				
	base [m]	2282.0		2292.0	2335.0		2650.0		2707.0	2814.0	2885.0			4411.0	4425.0	4530.0	4565.0	4615.0				
	N/G [-]	0.859		1.000	1.000		0.076		0.026	0.093	0.000			0.488	0.936	0.300	0.989	0.019				
G16-01	porosity [%]		17.55 ± 11.97																			
	top [m]	2460.0	2470.0																			
	base [m]	2470.0	2478.0																			
	N/G [-]	0.000	0.850																			
G18-01	porosity [%]																					8.80 ± 1.67 [2]
	top [m]																					3822.0
	base [m]																					3829.0
	N/G [-]																					0.357
L01-06	porosity [%]												0.68 ± 1.27	12.13 ± 1.43	14.63 ± 2.13	9.47 ± 2.70	14.21 ± 3.50	2.51 ± 1.76				1.26 ± 2.16
	top [m]												3008.0	3042.0	3055.0	3061.0	3125.0	3169.0				3899.0
	base [m]												3015.0	3055.0	3061.0	3125.0	3169.0	3392.0				3969.0
	N/G [-]												0.629	0.523	0.817	0.109	0.968	0.015				0.280
L02-02	porosity [%]	27.58 ± 2.12	21.39 ± 3.83						19.74 ± 1.59	21.12 ± 4.29	22.44 ± 4.07			3.43 ± 0.35	1.98 ± 1.21	4.98 ± 1.86	5.53 ± 2.94	0.77 ± 0.98				
	top [m]	2015.0	2094.0				2165.0		2188.0	2200.0	2276.0			3698.0	3733.0	3746.0	3892.0	3947.0				
	base [m]	2094.0	2165.0				2188.0		2200.0	2276.0	2445.0			3733.0	3746.0	3892.0	3947.0	4076.0				
	N/G [-]	0.853	0.942				0.000		0.075	0.193	0.222			0.009	1.000	0.264	0.985	0.022				
L02-04	porosity [%]	18.02 ± 1.69		15.65 ± 1.58	11.57 ± 1.91		15.94 ± 3.19		15.91 ± 4.42	18.03 ± 3.43	16.70 ± 5.24											
	top [m]	2006.0		2037.0	2049.0		2062.0		2100.0	2125.0	2200.0											
	base [m]	2037.0		2049.0	2062.0		2100.0		2125.0	2200.0	2450.0											
	N/G [-]	0.071		0.892	0.638		0.124		0.664	0.100	0.176											
L02-05	porosity [%]	36.46 ± 1.75		37.87 ± 2.19	28.1 ± 3.96		28.55 ± 4.73		25.94 ± 2.71	25.61 ± 3.84	19.65 ± 4.31			4.32 ± 0.84	10.92 ± 2.57	7.64 ± 2.65	9.83 ± 1.79 [1]					
	top [m]	1552.0		1567.0	1575.0		1611.0		1720.0	1748.0	1780.0			4016.0	4039.0	4052.0	4161.0	4200.0				
	base [m]	1567.0		1575.0	1611.0		1720.0		1748.0	1780.0	1953.0			4039.0	4052.0	4161.0	4200.0	4257.0				
	N/G [-]	1.000		1.000	1.000		0.911		0.993	0.309	0.316			0.043	1.000	0.196	0.975	0.000				
L02-07	porosity [%]	16.81 ± 0.58	22.86 ± 6.01								23.51 ± 1.30			8.84 ± 0.92	13.41 ± 1.35	8.5 ± 3.6	15.77 ± 4.18	4.33 ± 1.06				
	top [m]	1967.0	1982.0								2002.0			3889.0	3911.0	3925.0	4030.0	4071.0				
	base [m]	1982.0	2002.0								2014.0			3911.0	3925.0	4030.0	4071.0	4185.0				
	N/G [-]	0.027	0.330								0.250			0.032	0.957	0.223	0.993	0.025				
L03-01	porosity [%]	21.58 ± 1.38		18.56 ± 1.76	17.35 ± 2.91		19.59 ± 4.90		16.58 ± 3.85	13.18 ± 4.37	9.66 ± 5.08											
	top [m]	1822.0		1930.0	1946.0		2086.0		2399.0	2482.0	2674.0											
	base [m]	1930.0		1946.0	2086.0		2399.0		2482.0	2674.0	2990.0											
	N/G [-]	0.009		0.688	0.813		0.012		0.567	0.361	0.035											

Litho-stratigraphic units		SLSS	SLSG	SLSGS	SLSGP	SLCT	SLCTA	SLCTB	SLCTS	SLCTO	SLCF	SLCFR	RNSOF	RBMDC	RBMDL	RBMVC	RBMVL	RBSHR	ROCLT	ROSLU	ROCLA	ROSLL
L03-02	porosity [%]													9.9 ± 0.91	5.59 ± 2.21	5.63 ± 1.63	3.01 ± 2.73	4.37 ± 1.08				
	top [m]	2470.0		2497.0	2507.0		2620.0		2785.0		2860.0			4397.0	4419.0	4425.0	4513.0	4548.0				
	base [m]	2497.0		2507.0	2620.0		2785.0		2860.0		2936.0			4419.0	4425.0	4513.0	4548.0	4610.0				
	N/G [-]	0.056		0.580	0.905		0.048		0.575		0.037			0.023	0.800	0.442	0.974	0.008				
L03-04	porosity [%]	19.17 ± 3.94	10.28 ± 1.09				3.49 ± 1.74		13.76 ± 4.05	4.97 ± 6.07	8.08 ± 4.58			5.17 ± 0.43	6.91 ± 1.92	5.81 ± 2.00	10.08 ± 1.70	7.00 ± 1.53				
	top [m]	2247.0	2293.0				2432.0		2687.0	2726.0	2813.0			4063.0	4085.0	4118.0	4180.0	4210.0				
	base [m]	2293.0	2432.0				2687.0		2726.0	2813.0	2919.0			4085.0	4118.0	4180.0	4210.0	4258.0				
	N/G [-]	0.965	0.594				0.007		0.544	0.116	0.051			0.009	0.906	0.263	0.980	0.251				
L04-03	porosity [%]																					10.49 ± 2.78 [1]
	top [m]															2647.0	2695.0	2721.0				3697.0
	base [m]															2695.0	2721.0	2830.0				3776.0
	N/G [-]																					0.749
L05-01	porosity [%]	3.98 ± 3.09		1.08 ± 1.37	3.28 ± 3.90		8.06 ± 2.54				6.95 ± 5.54											
	top [m]	2770.0		2819.0	2825.0		2840.0				2855.0											
	base [m]	2819.0		2825.0	2840.0		2855.0				2981.0											
	N/G [-]	0.745		1.000	1.000		0.573				0.388											
L05-04	porosity [%]											19.75 ± 4.53										
	top [m]											2615.0										
	base [m]											2825.0										
	N/G [-]											0.112										
L06-01	porosity [%]		8.89 ± 4.53						5.17 ± 4.16				7.04 ± 3.08	7.52 ± 0.28	9.21 ± 2.40	6.74 ± 1.88	13.65 ± 2.40	11.11 ± 2.40				
	top [m]		3032.0				3145.0		3160.0				3707.0	3783.0	3804.0	3808.0	3903.0	3942.0				
	base [m]		3145.0				3160.0		3179.0				3715.0	3804.0	3808.0	3903.0	3942.0	4044.0				
	N/G [-]		0.767				0.000		0.853				1.000	0.029	0.900	0.383	1.000	0.020				
L06-02	porosity [%]	13.82 ± 1.09		11.8 ± 0.93	12.57 ± 1.28		4.92 ± 1.76		13.25 ± 5.39 [1,2]	1.14 ± 1.31 [2]	6.89 ± 4.36											
	top [m]	2105.0		2215.0	2226.0		2318.0		2463.0	2500.0	2565.0											
	base [m]	2215.0		2226.0	2318.0		2463.0		2500.0	2565.0	2733.0											
	N/G [-]	0.033		0.445	0.817		0.030		0.897	0.120	0.197											
L06-03	porosity [%]	25.81 ± 4.36	17.19 ± 2.00 [2]				18.44 ± 2.26		20.10 ± 7.44 [2]	18.66 ± 6.13	15.04 ± 6.17 [2]											
	top [m]	1991.0	2022.0				2048.0		2081.0	2175.0	2232.0											
	base [m]	2022.0	2048.0				2081.0		2175.0	2232.0	2342.0											
	N/G [-]	0.848	0.988				0.321		0.999	0.525	0.535											
L07-04	porosity [%]																		3.07 ± 1.16	8.39 ± 6.13	2.82 ± 2.24	9.75 ± 3.49
	top [m]												3183.0	3227.0	3244.0	3248.0	3332.0	3384.0	3842.0	3912.0	3982.0	4097.0
	base [m]												3186.0	3244.0	3248.0	3332.0	3384.0	3555.0	3912.0	3982.0	4097.0	4177.0
	N/G [-]																		0.023	0.380	0.155	0.958
L08-02	porosity [%]																					8.89 ± 4.08
	top [m]																	3366.0				4228.0
	base [m]																	3435.0				4289.0
	N/G [-]																					0.789
L08-03	porosity [%]																					8.47 ± 4.71
	top [m]													3390.0	3408.0	3414.0	3500.0	3548.0				4314.0
	base [m]													3408.0	3414.0	3500.0	3548.0	3658.0				4415.0
	N/G [-]																					0.757
L09-10	porosity [%]												22.25 ± 7.70 [2]	14.42 ± 3.06	19.84 ± 4.88	12.31 ± 2.85	22.9 ± 5.06	14.01 ± 2.35				
	top [m]												3080.0	3360.0	3375.0	3378.0	3436.0	3459.0				
	base [m]												3245.0	3375.0	3378.0	3436.0	3459.0	3512.0				
	N/G [-]												0.999	0.027	1.000	0.172	0.987	0.011				
L12-02	porosity [%]																		8.38 ± 4.65	13.53 ± 2.07 [1]	5.13 ± 1.76	4.51 ± 1.78
	top [m]																		2979.0	3034.0	3135.0	3204.0
	base [m]																		3034.0	3135.0	3204.0	3239.0
	N/G [-]																		0.184	0.872	0.171	0.471
L12-03	porosity [%]																		2.68 ± 1.23			
	top [m]																		2850.0	2912.0	2996.0	
	base [m]																		2912.0	2996.0	3120.0	
	N/G [-]																		0.348	0.749	0.263	

Litho-stratigraphic units		SLSS	SLSG	SLSGS	SLSGP	SLCT	SLCTA	SLCTB	SLCTS	SLCTO	SLCF	SLCFR	RNSOF	RBMDC	RBMDL	RBMVC	RBMVL	RBSHR	ROCLT	ROSLU	ROCLA	ROSLL
L12-05	porosity [%]																		4.60 ± 1.74	7.47 ± 5.56	4.58 ± 2.83	11.66 ± 2.42 [1]
	top [m]																		3136.0	3260.0	3279.0	3430.0
	base [m]																		3260.0	3279.0	3430.0	3438.0
	N/G [-]																		0.995	1.000	0.872	0.925
L15-01	porosity [%]																		8.73 ± 2.98	13.08 ± 3.83 [1]	4.78 ± 2.04	8.34 ± 2.55
	top [m]																		2832.0	2865.0	2989.0	3090.0
	base [m]																		2865.0	2989.0	3090.0	3099.0
	N/G [-]																		0.306	0.918	0.253	0.878
M01-01	porosity [%]	18.90 ± 2.41		10.60 ± 2.50	11.36 ± 1.30		12.24 ± 3.50		14.47 ± 1.52	10.85 ± 6.43	7.87 ± 6.43											
	top [m]	2032.0		2067.0	2084.0		2133.0		2285.0	2298.0	2356.0											
	base [m]	2067.0		2084.0	2133.0		2285.0		2298.0	2356.0	2437.0											
	N/G [-]	0.674		0.976	1.000		0.895		1.000	0.753	0.306											
M01-02	porosity [%]	9.69 ± 1.85		5.40 ± 1.12	6.55 ± 0.95		9.50 ± 1.09								8.99 ± 2.47	7.59 ± 1.43	12.32 ± 2.47 [1]	18.49 ± 2.28				
	top [m]	2650.0		2757.0	2769.0		2862.0		3019.0	3053.0	3114.0			3809.0	3829.0	3832.0	3917.0	3944.0				
	base [m]	2757.0		2769.0	2862.0		3019.0		3053.0	3114.0	3177.0			3829.0	3832.0	3917.0	3944.0	4004.0				
	N/G [-]	0.869		1.000	1.000		0.704		0.965	0.151	0.003			0.000	0.933	0.246	1.000	0.000				
M04-01	porosity [%]	15.53 ± 1.27	13.99 ± 2.78				7.33**		14.56 ± 5.40	15.61 ± 5.20	11.05 ± 6.84											
	top [m]	2720.0	2747.0				2789.0		2809.0	2825.0	2840.0											
	base [m]	2747.0	2789.0				2809.0		2825.0	2840.0	2978.0											
	N/G [-]	0.163	0.974				0.005		0.913	0.633	0.270											
M07-01	porosity [%]																		9.21 ± 2.53	13.93 ± 3.68	5.31 ± 1.45	6.78 ± 2.05
	top [m]																		3243.0	3416.0	3477.0	3460.0
	base [m]																		3416.0	3460.0	3561.0	3477.0
	N/G [-]																		0.325	0.911	0.320	0.612
M07-02	porosity [%]														16.74 ± 6.60	10.20 ± 3.88	10.74 ± 5.72 [2]	5.60 ± 3.82	3.67 ± 2.86	4.73 ± 1.91	1.64 ± 0.99	
	top [m]													2726.0	2734.0	2739.0	2798.0	2816.0	3098.0	3287.0	3342.0	3492.0
	base [m]													2734.0	2739.0	2798.0	2816.0	2915.0	3287.0	3342.0	3492.0	3499.0
	N/G [-]													0.000	0.780	0.137	0.967	0.020	0.374	0.485	0.253	
M08-01	porosity [%]																		8.24 ± 0.99	10.42 ± 1.93	9.07 ± 1.54	8.83 ± 2.30
	top [m]																		3298.0	3397.0	3505.0	3543.0
	base [m]																		3397.0	3505.0	3543.0	3621.0
	N/G [-]																		0.156	0.902	0.553	0.712
M10-02	porosity [%]																		2.73 ± 1.54	9.14 ± 4.36	5.28 ± 1.89	
	top [m]																		2715.0	2787.0	2904.0	
	base [m]																		2787.0	2904.0	3022.0	
	N/G [-]																		0.185	0.629	0.104	
M10-04	porosity [%]																		5.99 ± 1.21	6.27 ± 1.81	4.9 ± 1.42	
	top [m]																		2979.0	3065.0	3180.0	
	base [m]																		3065.0	3180.0	3298.0	
	N/G [-]																		0.450	0.578	0.293	
M11-01	porosity [%]																		5.97 ± 1.80	13.02 ± 1.69 [1]	4.53 ± 1.79	4.61 ± 1.68
	top [m]																		2694.0	2789.0	2910.0	2930.0
	base [m]																		2789.0	2910.0	2930.0	3036.0
	N/G [-]																		0.374	0.874	0.605	0.383

[1] *gas correction applied*

[2] *drilling core sample investigated*